Development of an ultrasound instrument for the assessment of skeletal maturity in beef carcasses

by

Jorge Antonio Simón

A Thesis Submitted to the

Graduate Faculty in Partial Fulfillment of the

Requirements for the Degree of

MASTER OF SCIENCE

Interdepartmental Program:	Biomedical Engineering
Department:	Electrical Engineering and Computer Engineering
Co-majors:	Biomedical Engineering
	Electrical Engineering

Iowa State University
Ames, Iowa

1994

TABLE OF CONTENTS

LIST OF FIGURES

LIST OF TABLES

CHAPTER 1. INTRODUCTION

Ultrasound applications have been extensively used in medicine, some areas of agriculture, animal sciences, and other areas. In the medical field, an ultrasound image can provide information about the size, shape and structure of an organ. Also, it can give information about the function of certain organs (e.g., heart, blood vessels) due to its ability to depict motion and flow (Doppler effect). In agriculture, ultrasound is used to evaluate many aspects of foods, such as the content or concentration of a specific food component, e.g., sugar in fruit juices, alcohol in wine, thickness of egg shells, and many more (Javanaud, 1988). In animal sciences, specifically in the meat industry, ultrasonic techniques have been used to determine fat thickness in beef cattle. More recently, there has been a growing interest in applying ultrasound to objectively grade beef in the carcass as well as in the live animal.

Ultrasound has been used in the beef industry for over 30 years, but for the past 11 years, the beef industry has been aiming towards an objective value-based system for beef grading (Cross and Whittaker, 1992). Ultrasonic parameters, such as speed of sound and attenuation, have been found to have great potential for the evaluation of materials' properties (Hsu and Hughes, 1992) and for tissue characterization (Whittaker *et al.*, 1992). These parameters

may make ultrasound technology a suitable grading tool to objectively determine the beef carcass value.

As a grading tool, ultrasound has some advantages over other methods used for tissue characterization, such as x-rays, imaging techniques, and histological techniques. First, ultrasound is non-invasive which means that the tissue under examination is not damaged, destroyed or irradiated and in most cases it does not need to be exposed for ultrasonic testing. Portability is the second advantage of ultrasound systems; the ultrasonic instrumentation takes very little space, and when combined with a portable computer, the system is adequate in portability and speed for an "on-line" evaluating system. Finally, ultrasonic instrumentation is relatively inexpensive as was demonstrated by Holland (1993) and Doerr (1992).

Among the ultrasonic grading systems, those based on A-Mode and B-Mode have shown the greatest potential of success (Cross and Whittaker, 1992). Marbling content and skeletal maturity are the factors used in the final determination of a USDA quality grade for a beef carcass (Boggs and Merkel, 1980). Most of the ultrasound research has been directed at determining the marbling content in the beef carcass (Anselmo *et al.*, 1987; Amin, 1989; Chang, 1991; Widyaatmadja, 1991; Doerr, 1992; Holland, 1993). The results obtained by the numerous researchers can be summarized by correlations between 60%

and 80%, which indicate that ultrasound holds great potential to objectively determine the marbling content.

However, it has been shown that eating quality characteristics such as tenderness, juiciness, and flavor are highly related to skeletal maturity (Tuma *et al.*, 1963; Boggs and Merkel, 1980). Therefore, a more objective method to assess skeletal maturity is needed.

Some of the current objective methods used to assess skeletal maturity are x-rays, histological techniques, and ultrasound. X-rays provide information about the atomic number density of the tissue being studied. Pezzoli and Bue. (1975) reported that it is possible to determine the degree of bone maturity by radiographic examination. Histological techniques are based on the determination of growth marks which are defined as the histological expression of any temporary time-dependent variation in bone growth rate. The results provided with this technique are the most reliable, but it is difficult to implement and to interpret the results (Castanet *et al.*, 1993). Finally, an early study performed by Davis *et al.* (1971) demonstrated that sound traveled through bone at a faster rate in the more mature samples. The correlation coefficient reported by Davis *et al.* was 74.9%. More recently, it has been shown that ultrasonic wave propagation is highly correlated with the microstructural units of bone when comparing young animals to old animals (Katz and Yoon, 1984).

The research described in this thesis involves the design and verification of a portable ultrasound system capable of estimating the speed of sound through bone samples from beef carcasses. The system was used to study the feasibility of using it to discriminate between different stages of skeletal maturity.

Objectives of Study

The purpose of the research described in this thesis was to investigate the feasibility to assess skeletal maturity (physiological age) in beef carcasses by measuring the speed of sound through bone. The specific objectives were:

- To design and develop an ultrasound device, based on the A-Mode pulse-through-transmission technique, suitable for bone samples.
- To calculate the speed of sound through bone samples of different known stages of skeletal maturity and relate it to the chronological age of the animal.
- To use the calculated physiological age to estimate the beef carcass maturity grade.

Thesis Organization

Chapter 2 reviews ultrasound basis and presents a brief overview about the beef grading process. Chapter 3 presents the system's design and the evaluation of the system's performance. It also describes the limitations of the system and the criteria used to select the bone samples to be used for this research. The reliability and validation of the system are presented in Chapter 4. This chapter also presents the results and discussion of the correlation studies between skeletal maturity and speed of sound through bone.

CHAPTER 2. BACKGROUND INFORMATION

Skeletal maturity constitutes an important factor in the process of determining the final beef grading. Ultrasound has been found to have a great potential in estimating the skeletal maturity The possibility of an objective method for estimating skeletal maturity would improve the actual subjective grading system used in the beef industry.. In order to better understand the applications of ultrasound as a beef grading tool, some pertinent background information in ultrasound, current beef grading procedures, and bone development and growth are given in this chapter.

Ultrasound

Sound audible to the human ear has a frequency in the range of 20 Hz to 20 KHz. Sound waves having frequencies above 20 KHz is termed ***ultrasound***. Sound of frequencies in the range of 1 MHz to 20 MHz are useful for medical applications, and for materials or tissue characterization.

Generation and detection of ultrasound

Generation and detection of ultrasonic waves can be achieved by several types of devices. The most common type used in medical applications is one that uses the so-called piezoelectric effect. Certain crystals have the property of

generating an electric voltage when compressed or expanded, and the voltage generated is proportional to the amount of compression/expansion applied to the crystal. Conversely, when an electric voltage is applied to a piezoelectric crystal, it changes its shape producing sound waves (Figure 2.1).

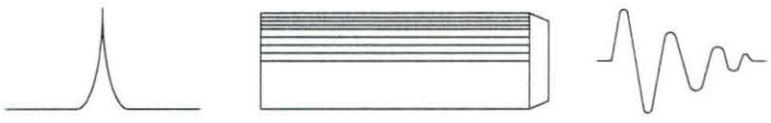

Figure 2.1: Piezoelectric effect: generation of a sound pulse by an electric impulse and *vice versa*.

Frequency characteristics of the transducer

The quality factor or Q-factor is a measure of the resonance characteristics of the transducer. It is defined as the ratio of the resonant frequency to the bandwidth (3 dB power). A transducer with a high Q-factor has a sharp resonance peak of narrow frequency response as shown in Figure 2.2a. Figure 2.2b shows that the bandwidth depends upon the pulse duration; the shorter the pulse duration, the broader the bandwidth.

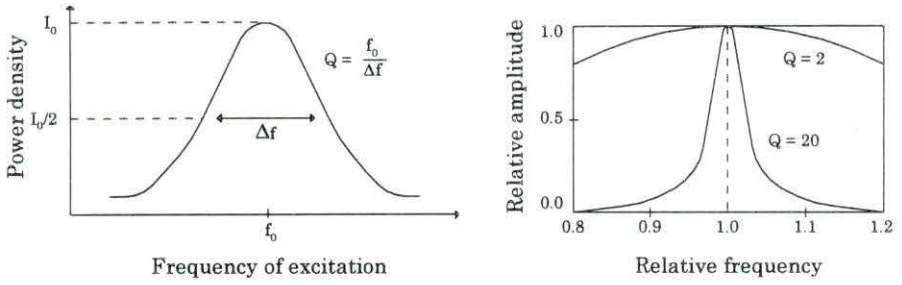

(a)

Pulse duration	Pulse waveform	Frequency spectrum	Spectral appearance
Long		Narrow	
Short		Broad	
Very short		Very broad	

(b)

Figure 2.2: Q-factor. Frequency characteristics of the transducer and pulsed ultrasound (Amin, 1989).

Axial or longitudinal resolution

The axial resolution of the system is given by the minimum distance between two objects that can be separately identified along a line in the direction of the sound wave. Axial resolution is limited by the pulse duration.

In Figure 2.3a, the two interfaces A and B are separated by a distance greater than one half the pulse duration. The echoes from A and B do not overlap and the transducer receives two separate echoes. In Figure 2.3b, A and B are closer together than one-half the pulse duration. In this case, the echoes overlap, and the transducer detects only one echo.

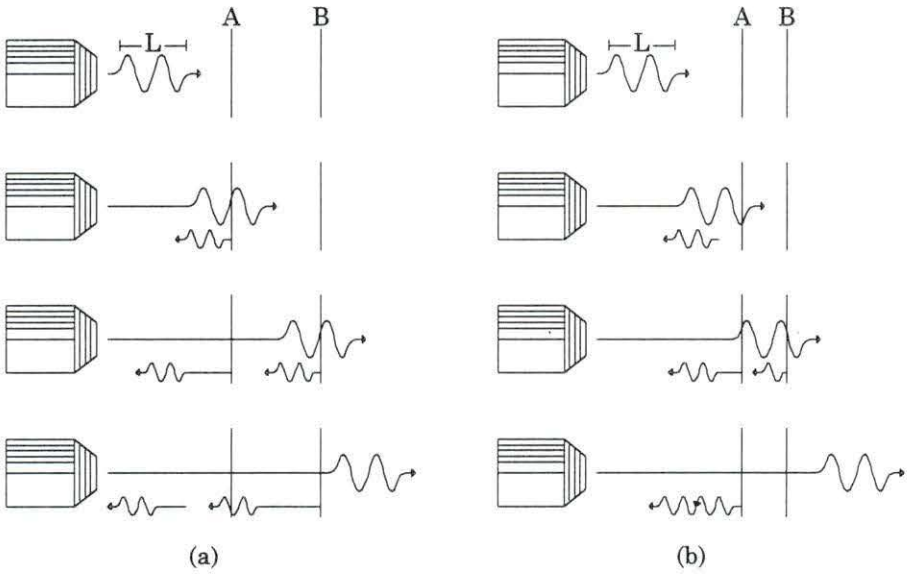

Figure 2.3: Axial resolution: the shorter the pulse duration is, the better is the axial resolution.

Lateral resolution

The lateral resolution is defined as the ability of the system to distinguish objects in a line perpendicular to the axis of the sound beam. The sound wave maintains the lateral dimensions of the transducer in the near field, but it starts

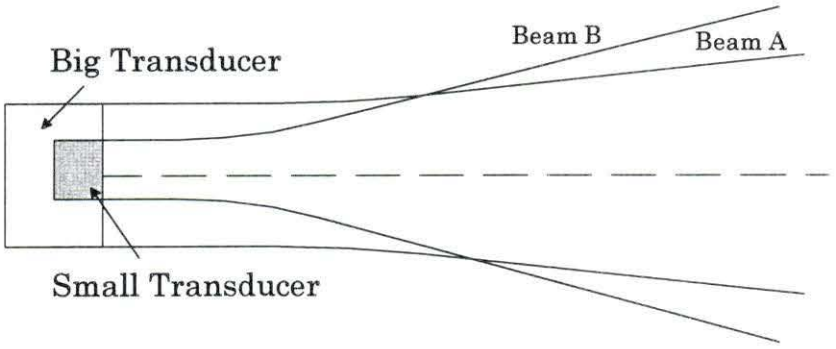

Figure 2.4: Lateral resolution. Beam profiles for two different size transducers, A and B (Smith, 1989).

to fan out in the far field. Figure 2.4 shows the beams for two transducers. Note that the smaller transducer's beam diverges more rapidly.

Speed of sound

The speed at which ultrasonic vibrations propagate in a medium depends on the physical properties of the material itself, such as the elasticity and the density. Therefore, it is an intrinsic property of the material. The wavelength of the propagating wave (λ) is directly proportional to the speed of sound (c) through the material and is inversely proportional to the resonance frequency of the transducer (f), as shown by the following equation:

$$\lambda = \frac{c}{f}$$

For example, a 1 MHz transducer used to diagnose soft tissue which has a characteristic speed of sound of 1540 m/s, provides a resolution of the tissue being studied of the order of 1mm.

Table 2.1 shows some biological media and their respective speeds of sound. It is important to note that the sound speed is highest in solids, somewhat lower in liquids and soft tissue, and very much lower in gases.

Table 2.1: Speed of sound in some biological media (Environmental Health Criteria, 1982)

Biological Medium	Sound Speed (m/s)
Bone (Skull)	4080
Brain	1540
Fat	1450-1490
Kidney	1565
Lens of eye	1600-1660
Lung	500-1000
Muscle (Skeletal)	1560-1600
Soft tissues	1510-1600
Water (20 °C)	1480
Water (50 °C)	1540

Speed of sound is an important parameter used to characterize some media or materials, e.g., the acoustical impedance, the modulus of elasticity, and other mechanical properties. In addition, speed of sound can be used to calculate the distance to a particular target in the medium or the thickness of the

material being studied. In the following equation:

$$V = \frac{d}{t}$$

the distance or thickness (d) and the time of flight (t) must be known in order to determine the longitudinal velocity (V). More generally, any two parameters must be known in order to obtain the third one.

Acoustic impedance and reflection

The resistance that the medium offers to a sound wave traveling through it is known as the acoustic impedance of the medium and is a property of the medium itself. Table 2.2 summarizes the characteristic acoustic impedances for some biological media.

Table 2.2: Acoustic impedance of some biological media (Hagen-Ansert, 1983)

Biological Medium	Acoustic Impedance ($Kg/m^2/sec$) x 10^6
Air	0.0004
Blood	1.6500
Bone (Skull)	7.8000
Fat	1.3400
Kidney	1.6300
Liver	1.6500
Lung	0.1800
Muscle	1.7100
Water	1.4800

The acoustic impedance can be calculated as the product of the speed of sound in the medium and the density of the medium. Whenever a sound beam passes an interface from a tissue of one acoustic impedance (Z_1) to another of different acoustic impedance (Z_2), a small proportion of the beam will be reflected back towards the transducer and the remainder will continue (refracted) in the forward direction (Figure 2.5).

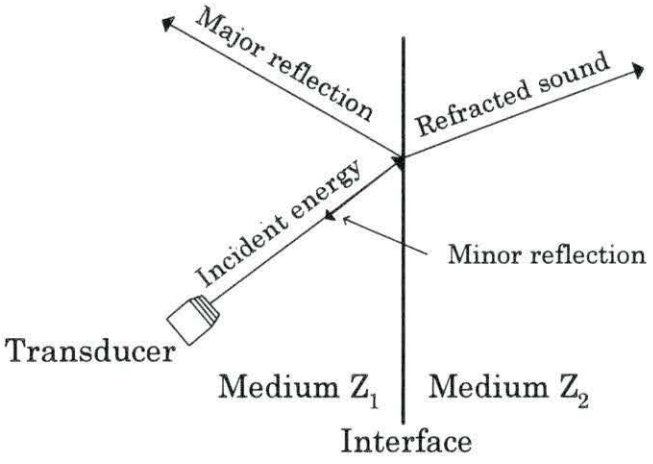

Figure 2.5: Reflective properties of an interface.

Attenuation

Sound energy is attenuated by the medium through which it travels as a result of interactions between the sound beam and the medium, these interactions include absorption, reflection, and scattering. Therefore, the amplitude and intensity of a sound beam is decreased as a function of the

distance traveled in the medium. The attenuation coefficient increases with increasing frequency, which limits the maximum frequency that can be used to study a particular medium. As an average "Rule of Thumb" the attenuation of an ultrasound beam in human soft tissue is 1 dB/cm/MHz (Wells, 1969). For example, for a structure at a depth of 10 cm, the attenuation is of the order 20 dB/MHz, since the signal has traveled twice the distance to the reflecting surface. For a 2 MHz transducer, this represents an attenuation of 40 dB.

Ultrasonic measurement techniques

The most common ultrasonic measurement techniques used in non-destructive evaluation of materials and tissue characterization are: pulse-echo and pulse-through-transmission. These techniques differ basically in the arrangement of the transmitter and receiver transducer and in the sitting position of the transducer on the surface of the material or tissue being tested. In the pulse-echo technique, the transmitter and the receiver transducers are placed close to the same point on the surface of the material (Figure 2.6a); sometimes the same transducer is used as both transmitter and receiver. In the pulse-through-transmission technique, the transmitter and the receiver are placed on parallel, opposite surfaces of the material. This technique requires two-sided access to the material or tissue being studied, as shown in Figure 2.6b.

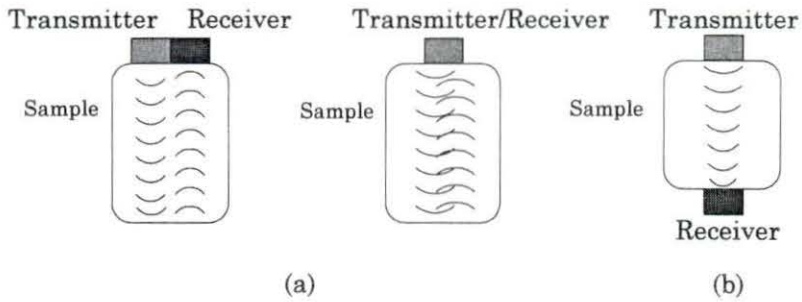

Figure 2.6: (a) Pulse-echo and (b) Pulse-through-transmission techniques (Whittaker *et al.*, 1992).

Display modes

Once the signal is received by the transducer and conditioned by the receiver amplifier, it is ready for display. The most common display modes are A-Mode and B-Mode.

A-Mode stands for amplitude-mode. A-Mode is a one-dimensional representation of the reflected echoes from an interface. One of the simplest ways to display these returning echoes is to use an **x-y** oscilloscope. The **x** axis represents time and the **y** axis is deflected in proportion to the amplitude of the echoes (Figure 2.7).

B-Mode stands for brightness-mode. The B-Mode represents the echo amplitudes of the A-Mode by bright spots of different intensity. Figure 2.8 shows the relationship between the A-Mode and B-Mode. The higher the amplitude is, the brighter the dot in the B-Mode representation.

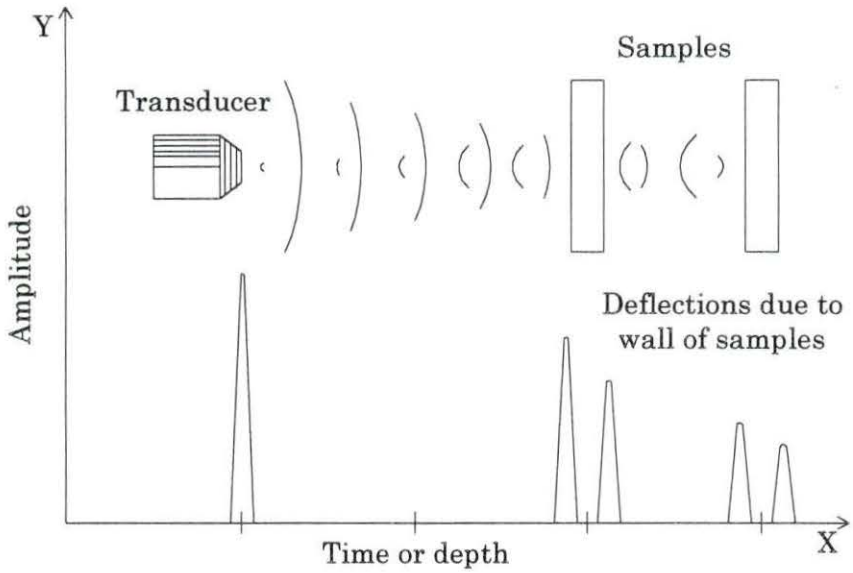

Figure 2.7: A-Mode display.

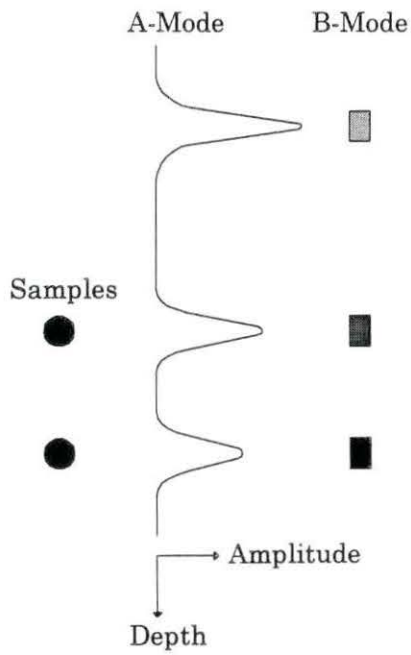

Figure 2.8: Relationship between A-Mode and B-Mode.

If the B-Mode is used to represent a series of reflected echoes from an interface, a 2-D representation (B-scan) of the test object can be displayed. The reflected echoes are taken at different angles on an arc, as shown in Figure 2.9. The rotation of the transducer is critical; it has to be fast enough to give a real time representation (real time scanners), and also it has to allow enough time for the echoes to return. The rotation of the transducer can be achieved by using mechanical elements attached to the crystal or by using electronic elements that delay the ultrasonic signal at each angle on the arc.

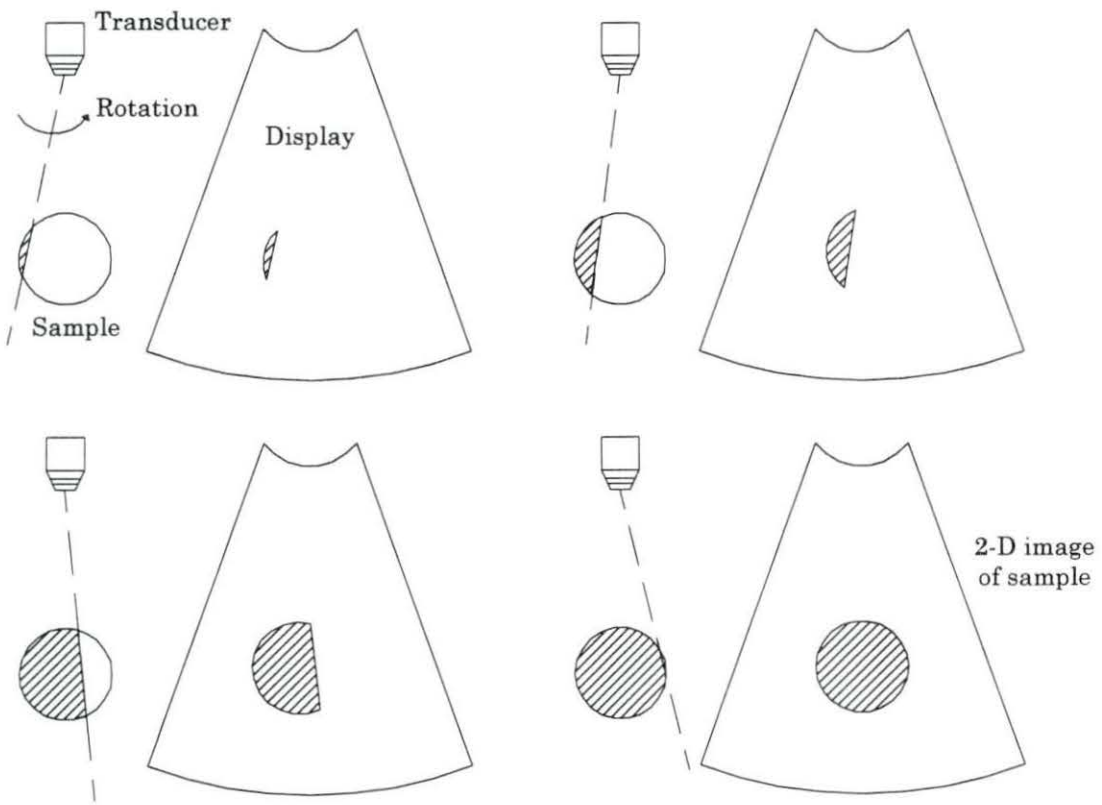

Figure 2.9: B-Mode. 2-D image development.

Beef Grading

Several factors are considered in determining the final beef carcass quality grade, e.g., degree of maturity, degree of marbling, and the color, texture, and firmness of lean in the ribeye muscle. Maturity and marbling are the two major factors. The combination of these two factors yields one of the following USDA beef quality grades: Prime, Choice, Select, Standard, Commercial, Utility, and Cutter (Boggs and Merkel, 1980).

Marbling

Marbling refers to the thin pockets of fat distributed in a cut of meat (intramuscular fat). It is estimated by examining the surface of the ribeye muscle between the 12^{th} and 13^{th} ribs. A highly trained USDA meat grader subjectively assigns the marbling score for a beef carcass. There are ten degrees of marbling score: abundant, moderately abundant, slightly abundant, moderate, modest, small, slight, traces, practically devoid, and devoid. Each of these is further divided into percentages in increments of 10% from 0% to 100%; the lowest marbling score is designated $degree^{0}$ and the highest $degree^{100}$ (Boggs and Merkel, 1980).

Maturity

Maturity refers to the physiological age of an animal rather than the chronological age. The major physiological indicators of maturity evaluated in the carcass are the bone characteristics and the ossification of cartilage Table B.1 in Appendix B summarizes the characteristics of the vertebrae and ribs with respect to maturity grades. Also, color and texture of the ribeye muscle are used as physiological indicators, since the muscle fibers increase in size and the color becomes darker with the aging process.

There are five maturity groups as shown in Figure 2.10. Each degree of maturity is designated by a letter with A being the youngest and E the oldest. Each of these is further subdivided into percentages in increments of 10% from 0% to 100%; the youngest degree of maturity for each group is designated *degree*^{0} and the oldest *degree*^{100} (Boggs and Merkel, 1980).

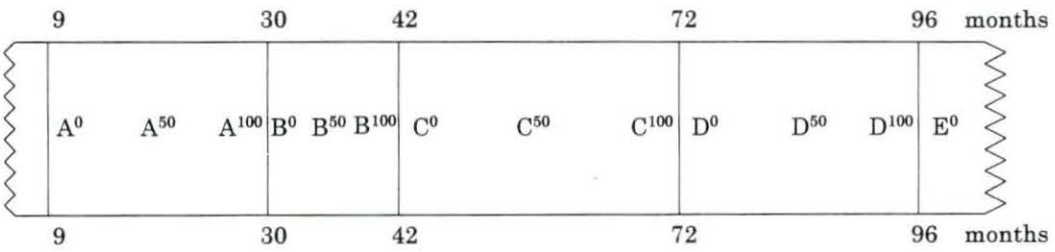

Figure 2.10: Range in months of age for each maturity grade (Boggs and Merkel, 1980).

The bones and cartilages evaluated in determining the physiological maturity of the beef carcass are those associated with the split backbone. More specifically, these are the sacral, lumbar and thoracic vertebrae, the cartilages between and on the dorsal edges of the individual sacral and lumbar vertebrae, and the "buttons" located on the dorsal tip of each spinous process of the thoracic vertebrae (Figure B.1). The upper four buttons (9th, 10 th, 11 th, and 12 th) of the thoracic vertebrae are given major attention in precisely determining the beef carcass's physiological maturity. Ossification of the cartilage in the sacral, lumbar, and thoracic regions does not occur simultaneously. It begins in the sacral region and progresses to the thoracic region with advancing age (Table B.1).

After the degree of marbling and skeletal maturity have been determined on a beef carcass, these two factors are combined to arrive at a final quality grade. Figure 2.11 shows the relationship of marbling and maturity to the final grade.

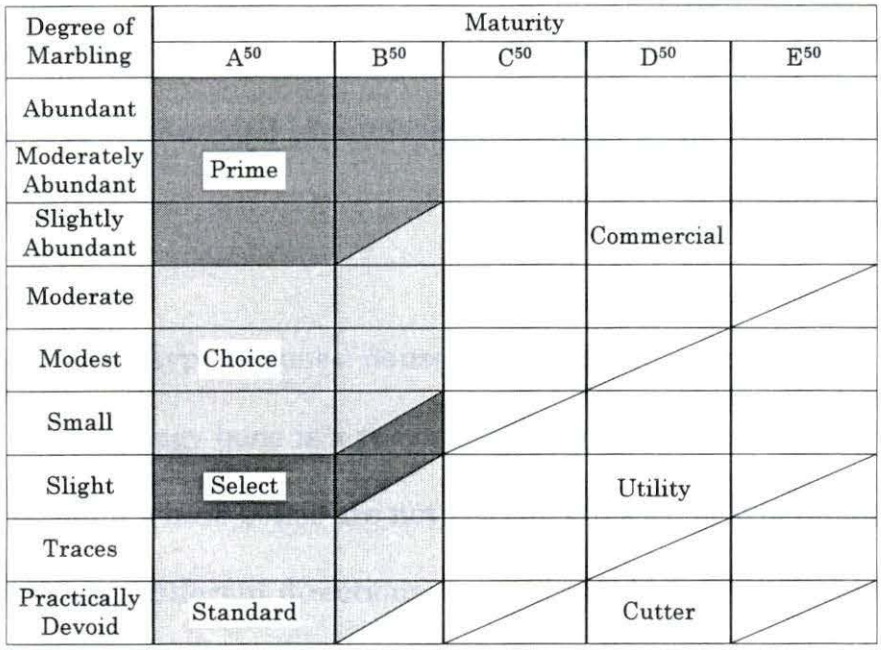

Figure 2.11: Relationship of marbling and maturity as used in determining final beef carcass quality grade (Boggs and Merkel, 1980).

Bone Growth and Development

Functions of bone

Bone provides **support** for the body against gravity, acting as a **lever** system for muscular action. **Protect** delicate and vital organs, i.e., the ribs protect the heart and lungs, the skull encloses the brain, the vertebrae shield the spinal cord, and the pelvis protect digestive and reproductive organs. Among its metabolic functions, **blood cell production** and **storage** are the most

important. Red blood cells are produced within the bone marrow. Calcium salts stored in bone represent a valuable mineral reserve that maintains normal concentrations of calcium and phosphate ions in body fluids (Martini, 1989).

Types of bone

There are two type of bones: dense or compact bone and spongy or cancellous bone. Spongy bone is a poorly organized tissue and randomly oriented; it is found where bones are not heavily stressed or where bones are stressed from many different directions, e. g., ribs and vertebrae. Compact bone, on the other hand, is a highly organized tissue and regularly oriented; it is found where stresses arrive from a limited range of directions, e. g., body of femur and humerus.

Bone Formation

Bone formation or ossification proceeds along two paths, endochondral or intramembranous. Intramembranous ossification initially resembles spongy bone, but the formation of additional matrix around the blood vessels can produce typical osteons. Bones produced in this manner are the roof of the skull, the lower jaw, and the clavicle. Endochondral ossification begins with the formation of a cartilaginous model then blood vessels penetrate the cartilage and

invade the central region and bone of the shaft becomes thicker. This type of ossification is characteristic of the long bones such as the humerus and femur.

The process of formation and destruction of bone continues throughout life as the osseous tissues undergo moulding and remoulding. During growth, deposition of bone tissue predominates over resorption. During adulthood, production and resorption of bone are balanced. Considerable variations exist in regard to the onset, intensity and distribution of age changes within individual bones, and among different individuals. As age advances, a deficit of osseous substance develops, which may be the result of inadequate formation of new bone or of increased resorption of old bone or a combination of both. This unbalance between bone formation and bone resorption accounts for the increased porosity and fragility of aged bones.

CHAPTER 3. INSTRUMENTATION

A portable ultrasound instrument was designed and implemented for the purpose of investigating its feasibility to assess skeletal maturity in beef carcasses. The instrument was developed using the A-Mode pulse-through-transmission technique. This chapter presents the features of the instrument as well as the evaluation of its performance according to the impulse response, the building cost, and the limitations.

System Design

The overall instrument design consists of five electronic sections and a set of transducers as shown in Figure 3.1.

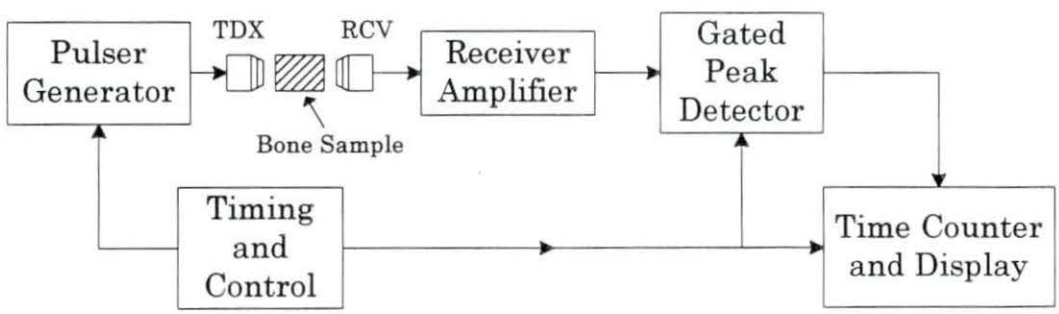

Figure 3.1: Overall block diagram of the ultrasound instrument.

The electronic sections are: 1) pulser generator, 2) receiver amplifier, 3) gated peak detector, 4) timing and control, and 5) time counter and display. The set of transmitter (TDX) and receiver (RCV) transducers is mounted on a calibrated caliper.

Each section was designed and individually tested to meet the design specifications (Figure A.1 in Appendix A shows a complete electrical schematic of the instrument). The specifications of the instrument are:

- The resonant frequency of the transmitter and receiver must be around 800 KHz to allow good penetration in bone tissue.
- The overall gain must be around 300 (50dB) to allow good echo detection.
- The system must be portable (battery operated).

Pulser generator

The pulser generator uses a low voltage mode pulser. The pulse energy is initially stored in the tuning inductor of the transmitter and is transferred to the transducer when the pulser is triggered. Figure 3.2 shows the circuit.

Two bipolar PNP transistors, Q1 and Q2, are used as a switch between the power supply (Vcc) and the transmitter transducer (TDX). The switch is driven by the output of U2A (74HC221), a dual non-retriggerable monostable

multivibrator (National Semiconductor, 1988), from the timing and control circuit. The output of U2A goes from "high" to "low" for 3.5μs, causing the transistors Q1 and Q2 to saturate (switch is closed), and current flows through the tuning inductor (L1). Then, the switch is opened and the energy stored in the magnetic field of the tuning inductor causes a large spike across the piezoelectric transducer (TDX) which then emits a burst of ultrasound.

The network formed by R1 and C1 speeds up the switching time of transistor Q2. The resistor R2 dampens the transducer to limit the number of oscillations and thus shortens the ultrasound pulse duration. The limiting network (R3, D1 and D2) prevents the receiver amplifier circuit from saturating due to the high voltage pulser spike. The voltage spike at the transmitter has an amplitude of about 40V and a rise time of approximately 100ηs (Figure 3.3).

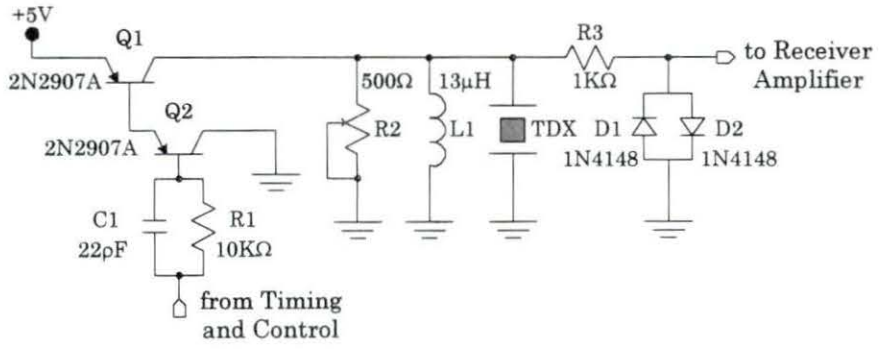

Figure 3.2: Schematic diagram of the pulser generator circuit.

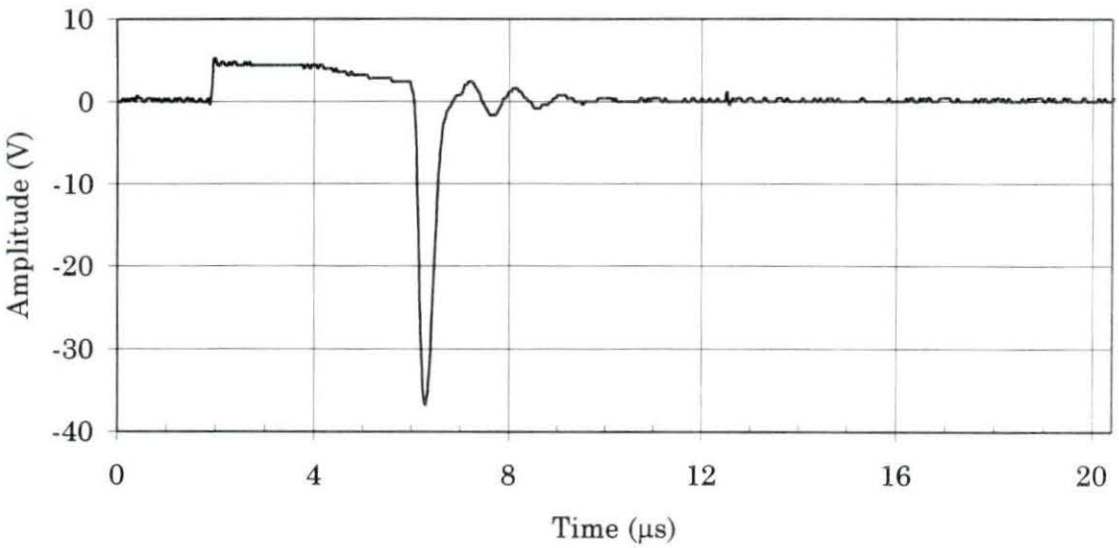

Figure 3.3: Electric impulse generated by the pulser generator to excite the transmitter transducer (TDX).

Receiver amplifier

The receiver amplifier circuit is designed to condition the reflected echoes received by the receiver transducer (RCV). The circuit uses a two-stage "cascode" amplifier with two bipolar NPN transistors, Q3 and Q4. The cascode configuration is commonly used in high frequency applications because of its ability to reduce the Miller effect (Boylestad and Nashelsky, 1978). The Miller effect is observed in single-stage transistor amplifiers, where there is a feedback between the input and the output through stray capacitance. The stray capacitance is amplified by the voltage gain of the circuit resulting in a

decreased bandwidth and voltage gain. The implemented cascode amplifier is shown in Figure 3.4.

The reflected echo received by the receiver transducer (RCV) is capacitively coupled to the common-emitter stage of the cascode amplifier (Q3). This stage provides a unity voltage gain which minimizes the stray capacitance. The second stage, the common-base section of the amplifier (Q4), provides a high voltage gain (45dB) which is given by resonance of the inductive load L2. The gain can be adjusted from 0 dB to 45dB by R4.

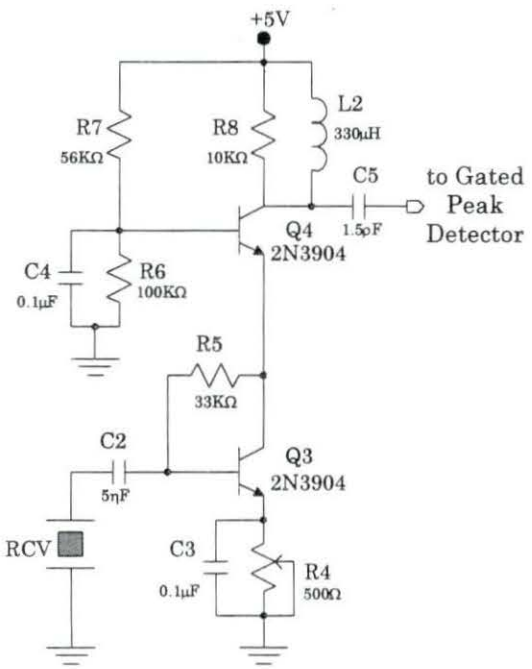

Figure 3.4: Schematic diagram of the receiver amplifier circuit.

Timing and control

This section provides all the control signals required for the pulser generator and the gated peak detector circuits to work properly as well as the timing signals for the time counter and display section. The schematic diagram of this circuit is shown in Figure 3.5.

This circuit is based on a CMOS timer U1 (LM555C), operating in the astable configuration with a clock frequency of 5KHz (T=200μs) and a duty cycle of 65% high and 35% low. The output is connected to the dual monostable multivibrator U2 (74HC221). The first monostable generates a pulse ($\overline{\text{SYN}}$) of width 3.5μs which is used to drive the pulser generator circuit and to start the time counter. It also generates SYN that is used to reset the counter U5B. The second monostable multivibrator is used to produce an adjustable delayed pulse (WDW) that is used to inhibit the main bang (pulser excitation) in the gated peak detector circuit and is set to 11μs.

Gated peak detector

The gated peak detector circuit is based on two high-speed, low-power voltage comparators U3 and U4, Maxim, MAX903 (Maxim, 1992). The gated peak detector circuit is shown in Figure 3.6.

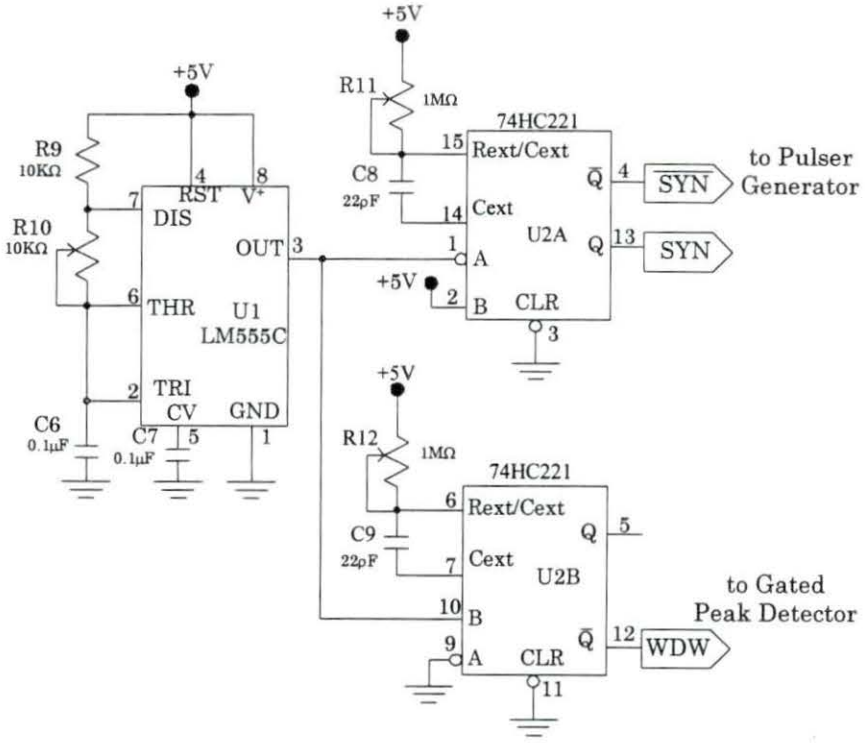

Figure 3.5: Schematic diagram of the timing and control circuit.

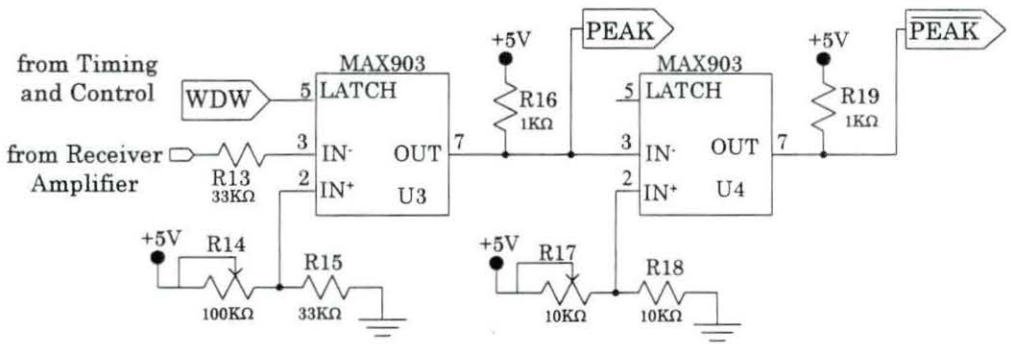

Figure 3.6: Schematic diagram of gated peak detector circuit.

The first comparator (U3) detects the first peak of the amplified received echo. The threshold level is set by the resistive network R14 and R15. The MAX903 voltage comparator has a built in latch which holds the output's state when the LATCH input (pin 5) is driven low. The LATCH input of U3 is used to inhibit the main bang produced by the pulser generator, and it is controlled by WDW, which is generated by U2B. The output of U3 (PEAK) is used to stop the counter in the time counter and display circuit . The second voltage comparator, U4, is used to invert the signal generated by U3. The output of U4 ($\overline{\text{PEAK}}$) resets the counter (U7) in the time counter and display circuit. The delay between PEAK and $\overline{\text{PEAK}}$ is less than 20ηs.

Time counter and display

The time counter and display section computes the time of flight of the ultrasound signal through the bone sample. It also provides an interface with the user by displaying the time on a liquid crystal display (LCD). The circuit diagram is shown in Figure 3.7.

Once the transmitter transducer is excited by ($\overline{\text{SYN}}$) triggering the pulser generator, the master clock (U6) starts running at a rate of 25 MHz, and it stops when a reflected echo is detected by the gated peak detector. The master clock (U6) is controlled by U5A (74HC390), a National Semiconductor dual 4-bit decade counter (National Semiconductor, 1988). Since the maximum clock

frequency of U8 (74C945), a National Semiconductor 4-digit LCD up/down counter/latch/decoder/driver (National Semiconductor, 1988), is 3MHz, U5B (74HC390), a 4-bit decade counter was used to divide the frequency of the master clock by 10. Thus, the input clock of U8 is 2.5 MHz. A National Semiconductor BCD-to-7 segment LCD latch/decoder/driver 74HC4543 (U7) is used to drive the first digit of the LCD. The LCD displays the final count of the counters (U5B and U8). A complete timing diagram is shown in Figure 3.8.

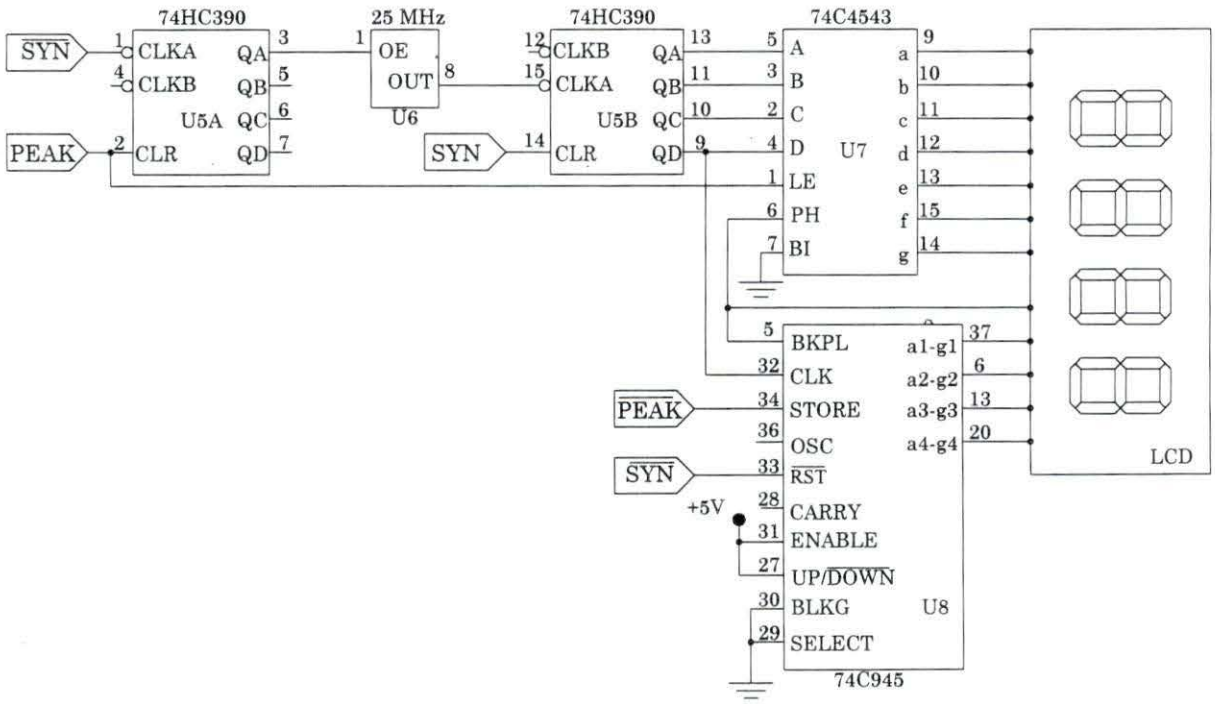

Figure 3.7: Schematic diagram of the time counter and display circuit.

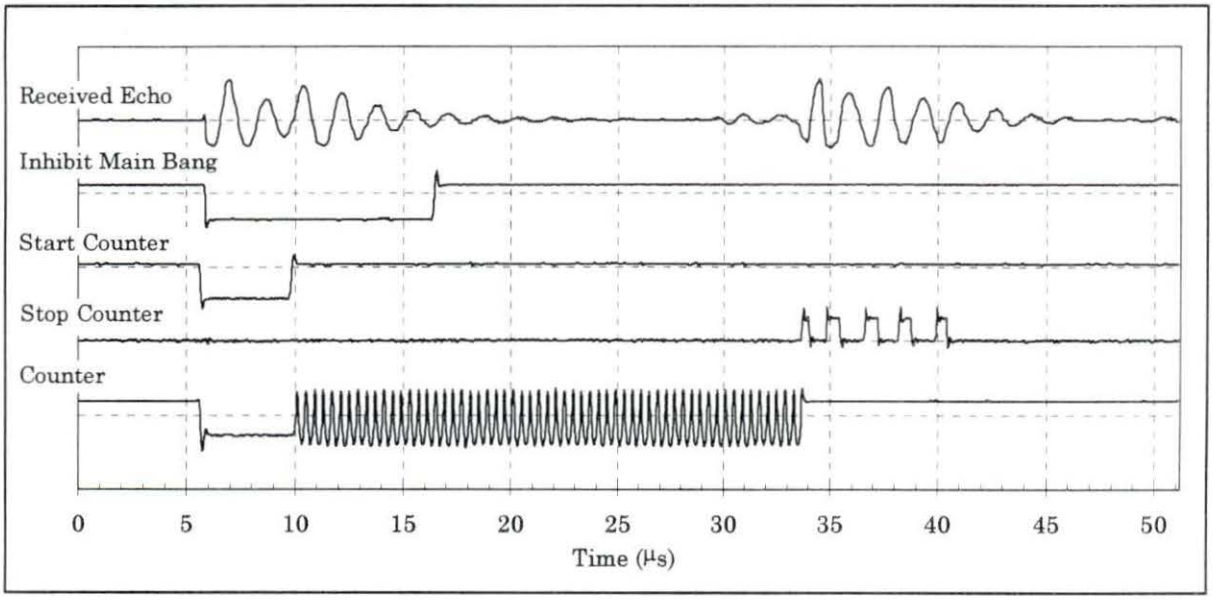

Figure 3.8: Timing diagram of the control signals for the time counter and display section.

Power supply

The instrument is powered by a single 9V alkaline battery to allow portability. The 9 V is DC-DC converted by a voltage regulator (LM78LS05) which generates a single power supply of +5V (Vcc). The drain on the battery by the instrument is less than 100 mA.

Set of transducers

The set of transducers used in this instrument are of PZT ceramic, inductively tuned to a center frequency of about 625KHz . One transducer is

used as a burst mode transmitter, and the other is used as an echo receiver. The set of transducers are mounted on a calibrated caliper from which the thickness of the sample is determined. The resolution of the caliper is 0.0005 inches (0.127 mm). The transducer assembly is shown in Figure 3.9.

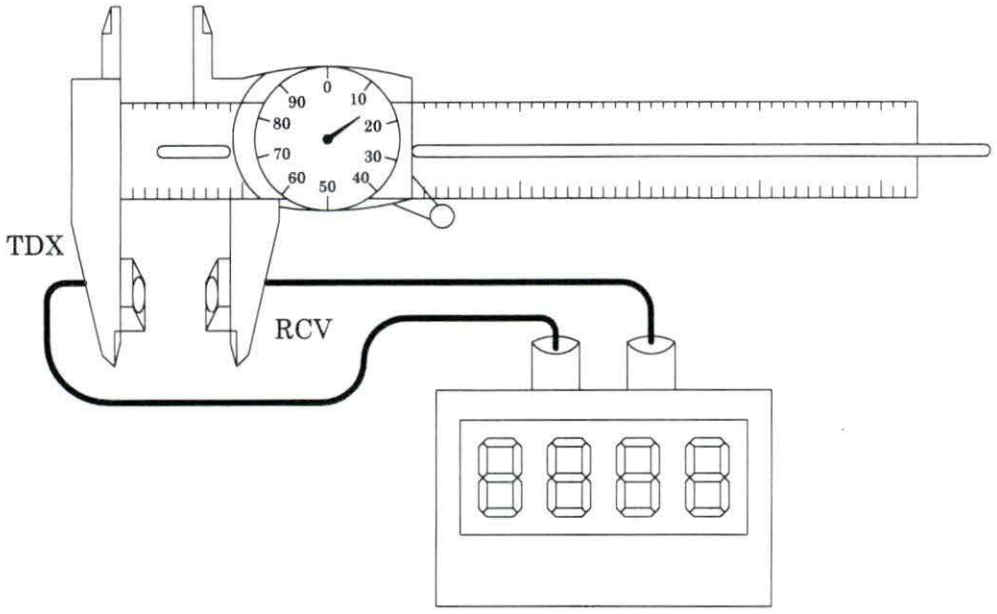

Figure 3.9: Assembly of the set of transducers, transmitter (TDX) and receiver (RCV), mounted on a calibrated caliper and connected to the ultrasonic instrument.

Instrument revisions

During the design process of the portable ultrasound system some problems were detected and several modifications were made before the final prototype was completed.

The first prototype used a voltage mode pulser with a high voltage power supply. The pulse generated with this pulser was appropriate to travel through bone samples, but the noise was such that the received signal was almost completely masked making peak detection very complicated. The noise was mainly introduced by the high frequency oscillating circuit of the high voltage power supply. This problem was solved by using a low voltage pulser generator as explained in the pulser generator section of this chapter.

Another modification was made on the gated peak detector circuitry. The voltage comparator used was a National Semiconductor LM301 which turned out to be too slow. The total delay introduced by the comparator was greater than 1μs. By using the fast voltage comparators, MAX903, the total delay became less than 50ηs.

Finally, the master clock frequency on the time counter and display section was increased from 20MHz to 25MHz. This change improved the resolution of the time counter by 10ηs for each count.

Measurement Technique

The ultrasound instrument uses the pulse-through-transmission technique with the transducers, transmitter and receiver, mounted on a calibrated caliper. The caliper is used to measure the thickness of the bone samples placed between the transducers. The bone samples are acoustically

coupled to the transducers by a water based gel. The instrument displays the time that a sound signal takes to travel from the transmitter through the bone sample to the receiver. Thus, the ratio of the sample thickness and the time of flight of the sound signal gives the characteristic speed of sound through the bone sample. In order to express the speed of sound through the bone in meters per second (m/s), the sample thickness measured with the caliper has to be converted from inches to meters (1 inch = 0.0254 m) and the time of flight given by the instrument has to be converted from counts to seconds (1 count = 40 ηs). Hence, the conversion factor used is given by the following equation:

$$V = \frac{d}{t} * 0.635 \text{ (m/s)}$$

where: d is the thickness of the bone measured in inches
t is the total counts displayed by the instrument

Instrument's Performance

The instrument's performance was evaluated by considering the impulse response of the set of transducers, the cost to build the instrument, and the limitations of the instrument. Based on these, appropriate bones were selected for further fine tuning of the system and experimentation.

Impulse response

The impulse response of the set of transducers was determined by digitizing the ultrasonic echo obtained by coupling a square piece of plastic of about 1 inch long between the set of transducers. The signal was digitized by using a digital oscilloscope (Tektronix 2232, Tektronix, OR). The time domain response was obtained by digitizing 1024 sample points at a sampling rate of 40ηs (Figure 3.10).

Figure 3.11 shows the frequency domain response obtained by taking the Fast Fourier Transform (FFT) of 512 sample points that corresponded to the received echo. The resonance frequency of the set of transducers is 625KHz and the 6 dB bandwidth is 150 KHz.

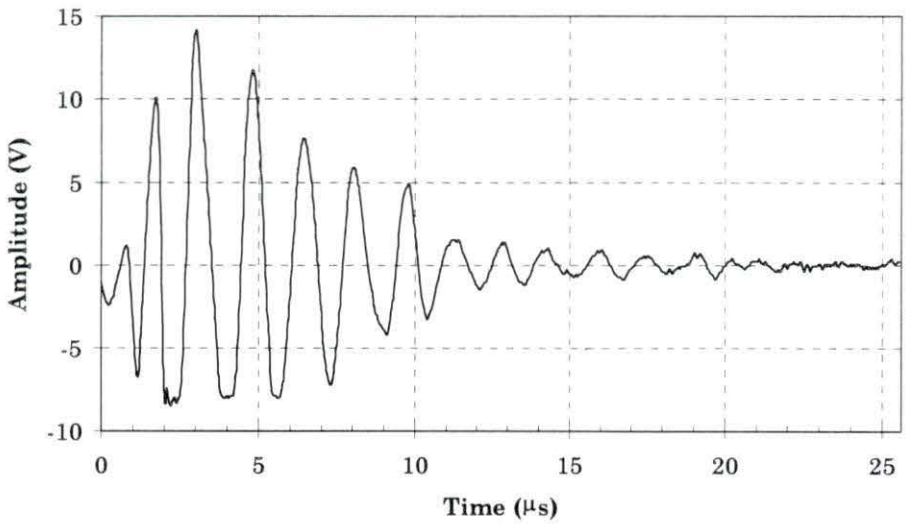

Figure 3.10: Received echo (512 sample points) used to calculate the frequency domain response of the set of transducers.

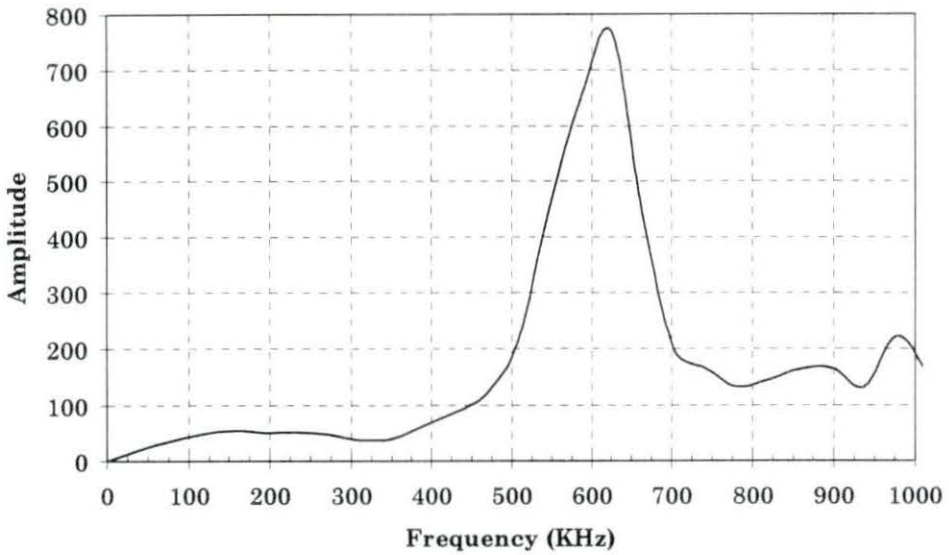

Figure 3.11: Frequency response of the set of transducers.

Cost

Appendix C (Table C.1) presents a list of the materials required to build the instrument, as well as an estimate of the cost of each item. The estimated cost was based on small purchasing orders of 10 components at a time. The total cost for the instrument hardware is $136.46. If the instrument were to be connected to a portable computer to perform the floating point calculations, the cost of the whole system would still be under $1000. The low instrumentation cost added to the potential that ultrasound has for tissue characterization makes this device a good choice for a grading tool.

Limitations of the instrument

Most of the limitations of the instrument were found in the assembly of the set of transducers and in the energy of the transmitted signal. These limitations are:

- Size of the bone sample. The bone sample has to be bigger than 0.5 inches and smaller than 2.0 inches. The lower limit is given by the excitation pulse of the transmitter transducer which rings for about 5μs above the threshold level set by the gated peak detector circuit. The upper limit is given by the high attenuation of the ultrasound signal through the bone sample.
- Geometry of the bone. The bone sample has to offer two flat parallel surfaces to the transducers, so a good acoustical coupling can be achieved, and the thickness of the sample can be accurately measured.

CHAPTER 4. RESULTS AND DISCUSSION

Once the final prototype of the instrument was built, several studies were conducted to select the most appropriate bones and to evaluate the repeatability and reliability of the measurements made by the designed system. Finally, different correlation studies were performed to evaluate the relationship between skeletal maturity expressed as age and the speed of sound through the bone samples.

Bone Selection

Different bones were collected from carcasses of unknown maturity at two meat packing plants and tested for their appropriateness according to the type of bone and the limitations of the instrument presented in the previous chapter. The following bones were tested:

- Femur
- Humerus
- Lumbar vertebrae
- Ribs
- Sacral vertebrae
- Scapula
- Thoracic vertebrae

Best results were obtained using the femur and humerus bones. These are long bones and their bodies contain mainly compact tissue, which makes the measurement of the longitudinal speed of sound easy and consistent. The other bone samples were discarded due to diverse inconveniences such as those previously mentioned in the instrument's limitation section. The scapula was discarded because its somewhat triangular shape failed to fit properly between the set of transducers. On the other hand, several attempts were made to use the ribs and the sacral, lumbar and thoracic vertebrae, because these bones reflect most of the skeletal changes with the aging process, but their trabecular structures contain numerous air pockets which increased the attenuation and the scattering of the ultrasonic signal. The received signal was extremely low; therefore, the measurements of speed of sound on these bones were very inconsistent and unreliable among different animals. Once the femur and the humerus bones were selected as the best choices, a fine tuning of the instrument was done with these bones for further experimentation.

Repeatability and Reliability of the Measurements

Once the instrument was fine tuned and the bones to be used were selected, the repeatability and reliability of the measurements were determined. The instrument's measurements were validated by comparing the results obtained to published ultrasound speed data from bovine femoral samples.

To determine the reliability of the measurements, three right femur bones from animals between 40 and 60 months old were used. The mid-diaphysis of each bone was sectioned into two pieces about 0.7 inches long. For each bone, 100 sound speed readings (50 for each piece of bone) were taken, so a total of 300 readings for the three animals were collected.

The ability of the instrument to yield consistent measurements of sound speed in the same bone was statistically determined by dividing all 100 readings from one bone into smaller groups according to the sample thickness, and making multiple comparisons between the groups by using the Duncan's multiple comparison test (Proc Glm/Means, SAS). First, descriptive statistics was used to analyze the differences among the means for each replicate. Table 4.1 shows that means and standard deviations for each replicate are very similar for each bone. The difference between the means may be due to the fact that the bones belong to animals of different skeletal maturities.

This informal statistical test showed that the measurements were very reliable (n=100, for each animal). A more formal test, Duncan's multiple comparison, was performed to assess differences among the measurements for each bone. All the readings from one animal were rearranged into groups according to their thickness in order to perform the test.

Table 4.1: Descriptive statistics for the repeatability and reliability study.

Sample	Bone 1		Bone 2		Bone 3	
	1	2	3	4	5	6
Mean (m/s)	2977	2975	3027	3026	2895	2890
Standard Deviation	35	35	33	49	29	36

Appendix D shows the rearranged data for all three bone samples (Table D.1) and a summary of the SAS output for this test (Figure D.1). Duncan's multiple comparison test showed that there was no significant difference among the measurements taken for any of the three bones studied. Thus, the instrument will likely yield the same results every time the sound speed through the same bone is measured.

In addition, the reliability of the measurements within a group and among groups was determined by the Cronbach's alpha (α) reliability coefficient, calculated by using the Correlation procedure (Proc Corr, SAS). This test measures the average correlation between groups and also the average correlation within a group. Cronbach's alpha reliability coefficient ranges from 0 to 1, the higher this coefficient, the more reliable the measurements. The result of this test showed that the sound speed measurements through bone samples taken with the instrument were highly reliable (α_{bone1}=0.896 , α_{bone2}=0.933, α_{bone3}=0.904) (Figure D.2).

Once the repeatability and reliability of the measurements were established, the sound speed readings were compared to published ultrasound speed data to determine the accuracy of the instrument. Table 4.2 shows published ultrasound speed data.

Sound speed measurements obtained throughout this research range from 2600 to 3400 (m/s) for different animals and various skeletal maturities. These ranges are highly comparable to those published for femoral bones. Thus, the instrument is effectively measuring the speed of sound through bone.

Table 4.2: Published ultrasound speed data on femoral bovine bone.

Reference	**Average Longitudinal Speed of Sound** (m/s)
Lang, Sidney. B. (1970)	3000-3800
Katz and Yoon (1984)	2750-3250
Williams, John L. (1991)	2800-3300
WHO. Ultrasound. (1982)	3000-3300
Webster, John G. (1992)	3360
Evans, F. G. (1973)	2660-3260

Assessment of Skeletal Maturity

To study the correlation between speed of sound and skeletal maturity, three experiments were performed. All bone samples were obtained from the Meat Laboratory in the Department of Animal Science at Iowa State University, and were collected after slaughter. Each long bone (femur and humerus) was sectioned transversely to its long axis with a band saw into three or four pieces ranging from 0.6 to 1 inch long depending on the length of the mid-diaphysis of each bone. After cutting, the bone pieces were refrigerated at 0°C and stored for 48 hours before ultrasonic testing was performed. The ultrasonic testing of the bone samples was completely randomized to avoid any biasing in the measurements.

Experiment one

This experiment used four animals of known maturity determined by a highly trained meat grader. Two animals were determined to be 15 months old while the other two were estimated to be 48 months old.

For the 15 months old animals, the right femur bones were cut into two pieces about 0.7 inches long for the first animal and into four pieces of the same size for the second one. A total of 10 readings were obtained for the first animal and 20 for the second one. For the 48 months old animals, the right femur bones

were cut into five pieces about 0.7 inches long for each animal. A total of 25 readings were obtained for each bone.

To determine the correlation between sound speed and skeletal maturity, two statistical tests were performed. First, a t-test assuming unequal variances (Proc Ttest, SAS) was performed to analyze significant differences in the sound speed measurements for the two groups (15 and 48 months). A significant difference ($p<0.0001$) was found between the two groups (Table D.2). As was expected, the speed of sound through the bone samples of the older animals (2918±63.5 m/s) was higher than that of the young animals (2506±146.4 m/s). Secondly, a linear regression was fit by using the Linear Regression Model (Proc Reg, SAS) to determine the degree of variability in skeletal maturity explained by the sound speed through bone (Table D.3). The simple correlation coefficient (r) between months of age and the sound speed through bone was 0.8915 accounting for 79.48% of the variability (R^2).

Experiment two

Ten right femur bones were obtained from 10 animals. The skeletal maturities were determined by a highly trained meat grader to be A^{50} (18 months), B^{0} (30 months), B^{50} (36 months), and C^{10} (45 months). Each bone was cut into four pieces about 1 inch long. Two sound speed readings were taken for each anatomical plane of the bone samples: caudal, cranial, lateral, and medial.

Therefore, 32 readings were taken for each bone, and a total of 320 readings for the 10 animals were collected. A Duncan's multiple comparison test (Proc Glm/Means, SAS) was performed to determine the differences among the sound speed measurements at different anatomical planes (caudal, cranial, lateral, and medial) and at different stages of skeletal maturities (Figure D.3). Multiple comparisons of the sound speed measured at different anatomical planes revealed that those measured at the cranial plane were significantly higher than those for the other planes. These results are in agreement with those found by Katz and Yoon (1984), but in their research, they also found differences in the medial plane. On the other hand, the result of the multiple comparison by age revealed that there were significant differences between the 36 months old and the 18 months old animals. No significant difference was found among the 30, 36, and 45 months old animals. From the previous test, nothing can be concluded about the relationship between the speed of sound through the bone and the skeletal maturity. Figure 4.1 shows a 3-D plot of age, average sound speed through bone by age, and anatomical planes.

A random pattern governs the relationship of sound speed and anatomical plane with skeletal maturity. Even though the relationship between age and sound speed is not apparent from the previous analysis, their relationship is

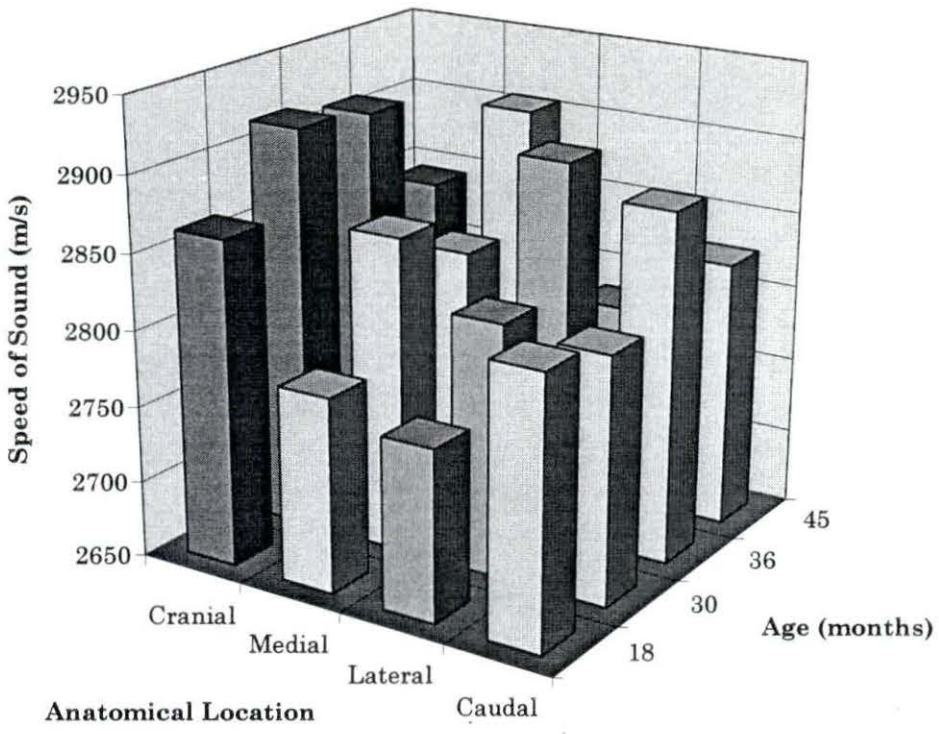

Figure 4.1: Relationship between age (skeletal maturity), sound speed, and anatomical planes.

clear when the average sound speed among the 10 animals is plotted versus age (Figure 4.2). In this experiment, the speed of sound for older animals was higher than that for younger animals, with the exception of the 45 months old animals which was even lower than the 30 months old animals, as shown in Table 4.3.

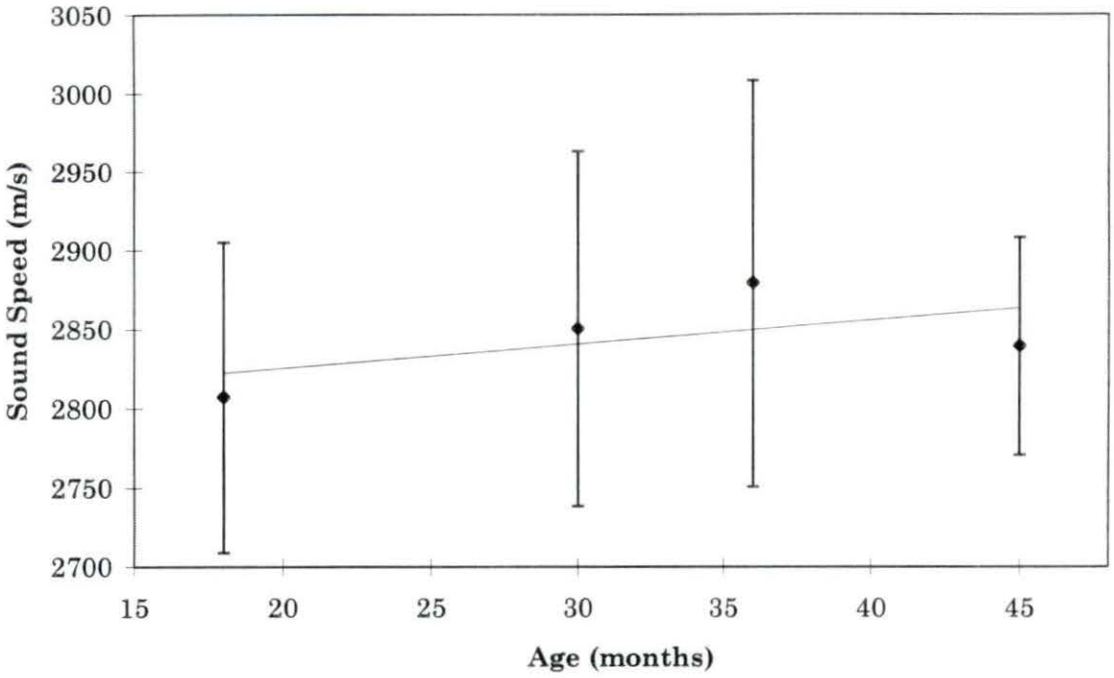

Figure 4.2: On average relationship between age (skeletal maturity) and speed of sound through bone.

Table 4.3: Descriptive statistics of the relationship between average sound speed (by anatomical plane) and age.

Estimated Age	18 months	30 months	36 months	45 months
Average Sound Speed (m/s)	2807	2851	2879	2840
Standard Deviation	98	112	128	69

Experiment three

The right and left femur and humerus bones of five animals of known chronological ages were collected. The age of the animals were 12, 13, 19, and 31 months old. Each bone was cut into four pieces about 1 inch long (when possible). A total of 16 readings were obtained from each bone; four readings from each piece. For this experiment, the live weight of each animal was also recorded. Table 4.4 shows the chronological age, live weight and the final quality grade for each animal.

Table 4.4: Characteristics of the animals used for experiment three.

Chronological Age	Live Weight	Quality Grade
12 months	1095 lb	Select$^-$
13 months	954 lb	Choice$^-$
13 months	1015 lb	Select$^+$
19 months	1265 lb	Choice$^-$
31 months	1430 lb	Com$^-$

In this experiment, the sound speed through the bone samples and the live weight of the animals were included in a linear regression model to predict the age of the animals by using the Linear Regression Model (Proc Reg, SAS). The following equation was used:

$$\hat{Age} = \beta_0 + \beta_1 * Sound\ Speed + \beta_2 * Live\ Weight$$

The explained variability (R2), the number of samples (n), and the prediction equation for each of the bones analyzed in this experiment are presented in Table 4.5.

A summary of the linear regressions for the right humerus, left humerus, right femur, and left femur are presented in Table D.4, Table D.5, Table D.6, and Table D.7, respectively. The speed of sound through the bone and the live weight of the animals were statistically significant for the linear models to predict age. The level of significance for the live weight was lower ($p<0.0001$) than that for the speed of sound ($p<0.02$, the highest). For each bone sample, predicted age calculated by the linear regression was plotted against the known chronological age to validate the linear equations obtained. These plots are shown in Figure 4.3, Figure 4.4, Figure 4.5, and Figure 4.6.

Table 4.5: Linear relationship between sound speed, live weight and age (skeletal maturity).

Bone	n	R^2	Prediction Equation
Right Humerus	60	89.13%	$\hat{Age} = -56.877 + 0.014 * Sound\ Speed + 0.029 * Live\ Weight$
Left Humerus	50	85.54%	$\hat{Age} = -49.669 + 0.009 * Sound\ Speed + 0.034 * Live\ Weight$
Right Femur	80	87.44%	$\hat{Age} = -60.897 + 0.014 * Sound\ Speed + 0.033 * Live\ Weight$
Left Femur	80	86.24%	$\hat{Age} = -48.865 + 0.011 * Sound\ Speed + 0.030 * Live\ Weight$

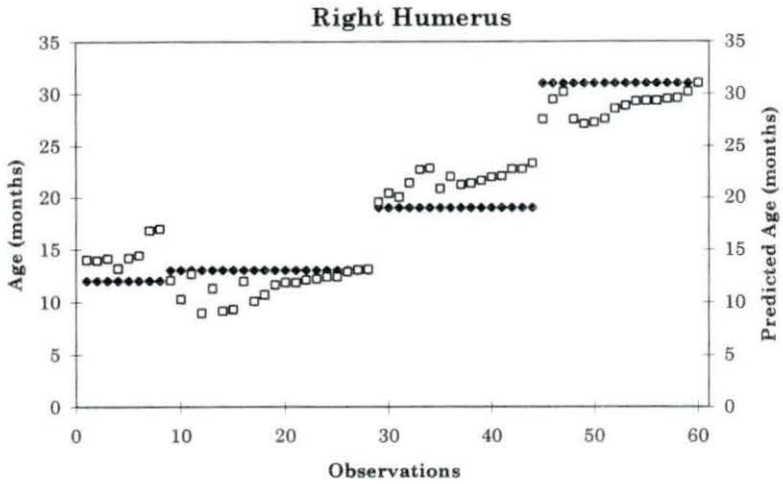

Figure 4.3: Plot of the chronological age versus the predicted age in the right humerus.

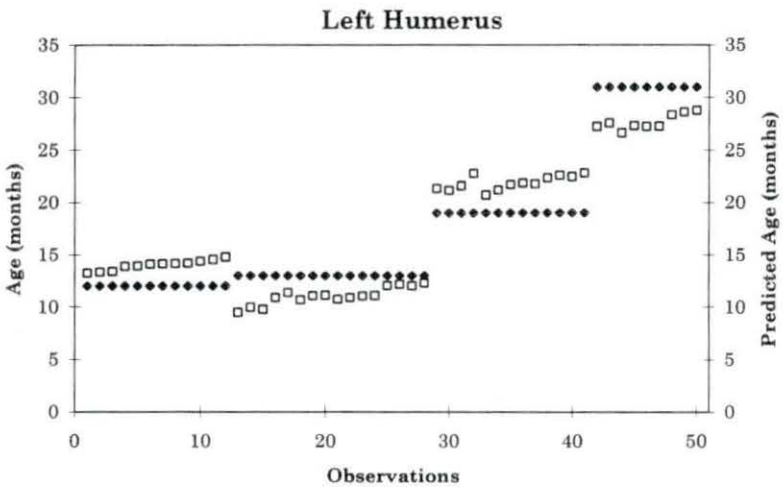

Figure 4.4: Plot of the chronological age versus the predicted age in the left humerus.

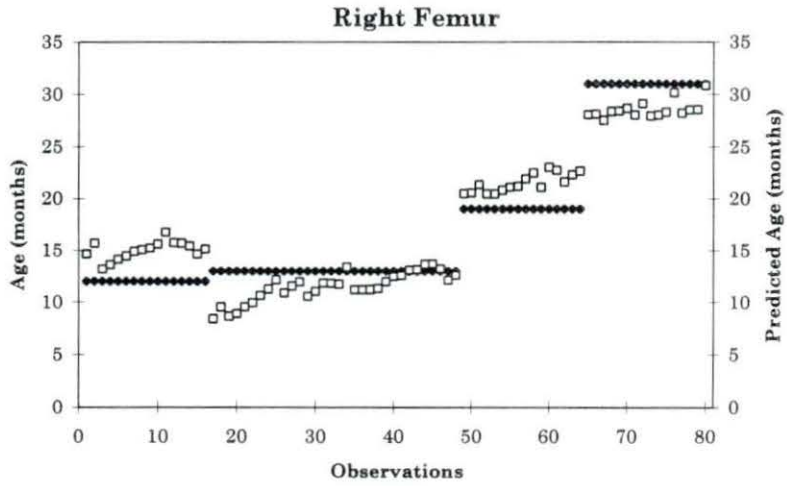

Figure 4.5: Plot of the chronological age versus the predicted age in the right femur.

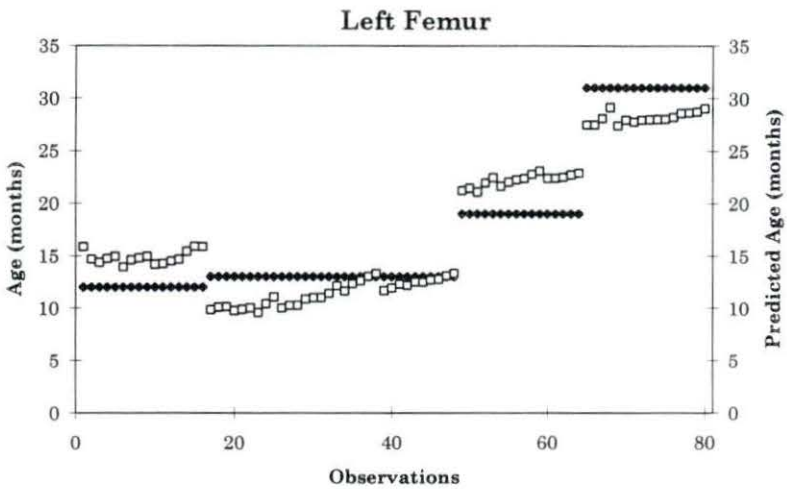

Figure 4.6: Plot of the chronological age versus the predicted age in the left femur.

Discussion

The instrumentation developed has shown that an inexpensive and portable A-Mode ultrasound system can perform well when used for the assessment of skeletal maturity in beef carcasses.

The results obtained in this limited study show that a definitive relationship exist between speed of sound through bone, animal live weight and skeletal maturity. The high correlation coefficients obtained for each of the linear prediction equations in experiment three and the linear trends shown in experiments one and two indicate that ultrasonic speed measurements have great potential to objectively assess skeletal maturity in beef carcasses.

In all experiments, the speed of sound measured through more mature bones was higher than that through less mature bones. In addition, the prediction models obtained in experiment three revealed that there are significant differences between anatomical age and physiological age. This difference can be seen in Figures 4-3 to 6, where the predicted age for the 12 months old animal was even hingher than that for the two 13 months old animlas. The predicted physiological age calculated by the prediction models was in close agreement to the final beef carcass quality grade for each animal.

Recommendations

To improve the potential of using speed of sound measurements through bone to determine skeletal maturity and final quality grade in beef carcasses, the following recommendations might be taken into account.

1. The energy of the transmitted ultrasound signal should be increased. This will allow an increase in the resonant frequency of the transducers which will have a direct effect on the resolution of the received signal, and consequently on the determination of the time of flight of the signal through the bone sample. This change will also reduce the variability among the measurements.
2. Using a more sophisticated device to measure the thickness of the bone samples. Such a device can be infrared or ultrasonic based. The device can feed the measured thickness into a computer for further calculation of the sound speed through the bone sample. This change will also reduce the variability among the measurements.
3. Controlling the breed and gender of the animals to be used for testing. Since it is known that sexual hormones influence bone formation and destruction (Cowin, 1989), better results would be obtained by controlling the gender. Also, there are considerable variations among animals' breed (Boggs and Merkel, 1980). The prediction models

constructed by using just one breed and one gender would be more accurate due to the reduction of the variability on the measurements.

These changes would increase the potential of the instrument to be implemented in an "on-line" basis for skeletal maturity assessment.

BIBLIOGRAPHY

Amin, Viren. 1989. Ultrasonic attenuation estimation for tissue characterization. M.S. Thesis. Iowa State University. Ames.

Anselmo, V. J., J. Clark and P. M. Gammell. 1987. Electronic inspection of beef. JPL invention report NPO-15477/4352. NASA Tech Brief 11(6) Item #67:1. (Jet Propulsion Laboratory, California Institute of Technology, Pasadena, California).

Boggs, D. L. and A. M. Merkel. 1980. Live animal carcass evaluation and selection manual. Kendall/Hunt, Toronto. pp 83-96

Boylestad, P. and L. Nashelsky. 1978. Electronic devices and circuit theory. Prentice Hall, Englewood Cliffs, New Jersey. pp 343-345

Castanet, J., H. Francillon-Vieillot, F. J. Meunier, and A. De Ricqles. 1993. Bone and individual aging. Bone Growth-B. Vol. 7. 9:245-277

Chang, Alan. 1991. Utility of the backscattered ultrasound A-Mode signal for the quantitative grading of beef. M.S. Thesis. Iowa State University. Ames.

Cowin, Stephen C. 1989. Bone mechanics. CRC Press, Florida. pp 2-11

Cross, H. R. and A. D. Whittaker. 1992. The role of instrument grading in a beef value-based marketing system. Journal of Animal Science 70:984-989

Davis, C. E., E. E. Finney, and D. R. Massie. 1971. Use of sonic and ultrasonic measurements on bovine bone to estimate chronological age. Journal of Food Science 36:141-143

Doerr, Vincent. 1992. Portable high speed data acquisition system for ultrasound tissue characterization. M.S. Thesis. Iowa State University. Ames.

Environmental Health Criteria 22. 1982. Ultrasound. World Health Organization. Geneva. 35pp.

Evans, F. Gaynor. 1973. Mechanical properties of bone. Charles C. Thomas, Illinois. pp 167-168

Hagen-Ansert, Sandra L. 1983. Textbook of diagnostic ultrasonography. C.V. Mosby Company, St. Louis. pp 8-9

Holland, Kyle. 1993. A field portable ultrasound system for bovine tissue characterization. Ph. D. Dissertation. Iowa State University. Ames.

Hsu, David K. and M. S. Hughes. 1992. Simultaneous ultrasonic velocity and sample thickness measurements and application in composites. Journal of Acoustical Society of America 92:2-669

Javanaud, C. 1988. Applications of ultrasound to food systems. Ultrasonics 26:117-123

Katz, J.L. and H.S. Yoon. 1984. The structure and anisotropic mechanical properties of bone. IEEE Transactions on Biomedical Engineering. Vol. BME-31, No. 12 878

Lang, Sidney B. 1970. Ultrasonic method for measuring elastic coefficients of bone and results on fresh and dried bovine bones. IEEE Transactions on Biomedical Engineering Vol. BME-17, No. 2 101

Martini, Frederick. 1989. Fundamentals of anatomy and physiology. Prentice-Hall, Englewood Cliffs, New Jersey. pp 157-165

Maxim. 1992. New releases data book. Technical notes 19-2887. Rev. 3, 11/92. Sunnyvale, California.

National Semiconductor. 1987. Linear data book (Vol. 1). Santa Clara, California.

National Semiconductor. 1988. CMOS logic data book. Santa Clara, California.

Pezzoli, G., and M. Bue. 1975. Radiographic evaluation of skeletal development in trotting horses in relation to their athletic activity. Folia veterinaria latina. 5:3,399-411

Romans, J. R., W. J. Castello, C. W. Carlson, M. L. Greaser and K. W. Jones. 1994. The meat we eat. Interstate Inc. Illinois. pp 544

Smith, Anne M. 1989. Personal computer based instrumentation for ultrasonic tissue characterization. M.S. thesis. Iowa State University. Ames.

Tuma, H. J., R. L. Hendrickson, G. V. Odell and D. F. Stephens. 1963. Variation in the physical and chemical characteristics of the longuisimus dorsi muscle from animals differing in age. Journal of Animal Science 22:354

Webster, John G. 1992. Medical instrumentation. Application and design. Second edition. Houghton Mifflin, Boston, 684pp.

Wells P.N.T. 1969. Physical principles in ultrasonic diagnosis. Academic Press, New York, 12pp

Whittaker, A. D., B. Park, B. R. Thane, R.K. Miller, and J.W. Savell. 1992. Principles of ultrasound and measurement of intramuscular fat. Journal of Animal Science 70:942-952

Widyaatmadja, Lanny. 1991. Attenuation measurement of the backscattered ultrasound A-Mode signal for beef grading. M.S. Thesis. Iowa State University. Ames.

Williams, John L. 1991. Ultrasonic wave propagation in cancellous and cortical bone: Prediction of some experimental results by Biot's theory. Journal of Acoustical Society of America 91:2-1106

ACKNOWLEDGMENTS

I would like to acknowledge Iowa Beef Industry Council for partial funding of this research. I would also like to express my deepest gratitude to the Biomedical Engineering Department, especially Dr. Mary Helen Greer, for all the support and encouragement during my graduate studies at Iowa State University.

I express my sincere thanks to my major professor Dr. David Carlson for giving me the opportunity to work with him in this research. I am also indebted to Dr. F. C. Parrish and Dr. Bob Johnson for arranging field trips and collecting bone samples for this research. I also thank Dr. Curran Swift, F. C. Parrish and Dr. Nany Goshal for serving in my committee

APPENDIX A

SCHEMATIC DIAGRAM OF THE SYSTEM

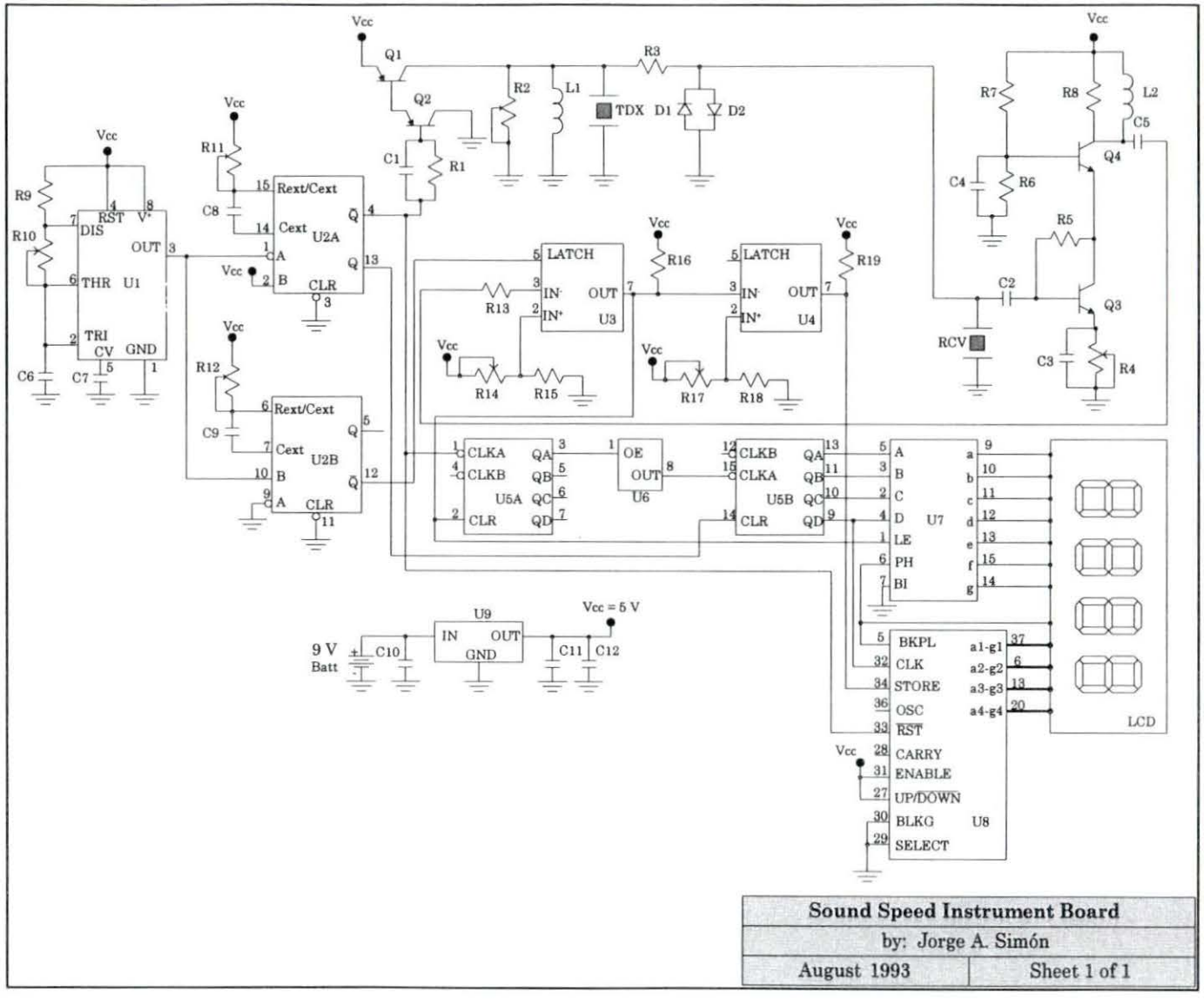

Table A.1: Complete electrical schematic of the instrument

APPENDIX B

SKELETAL CHARACTERISTICS OF A BEEF CARCASS

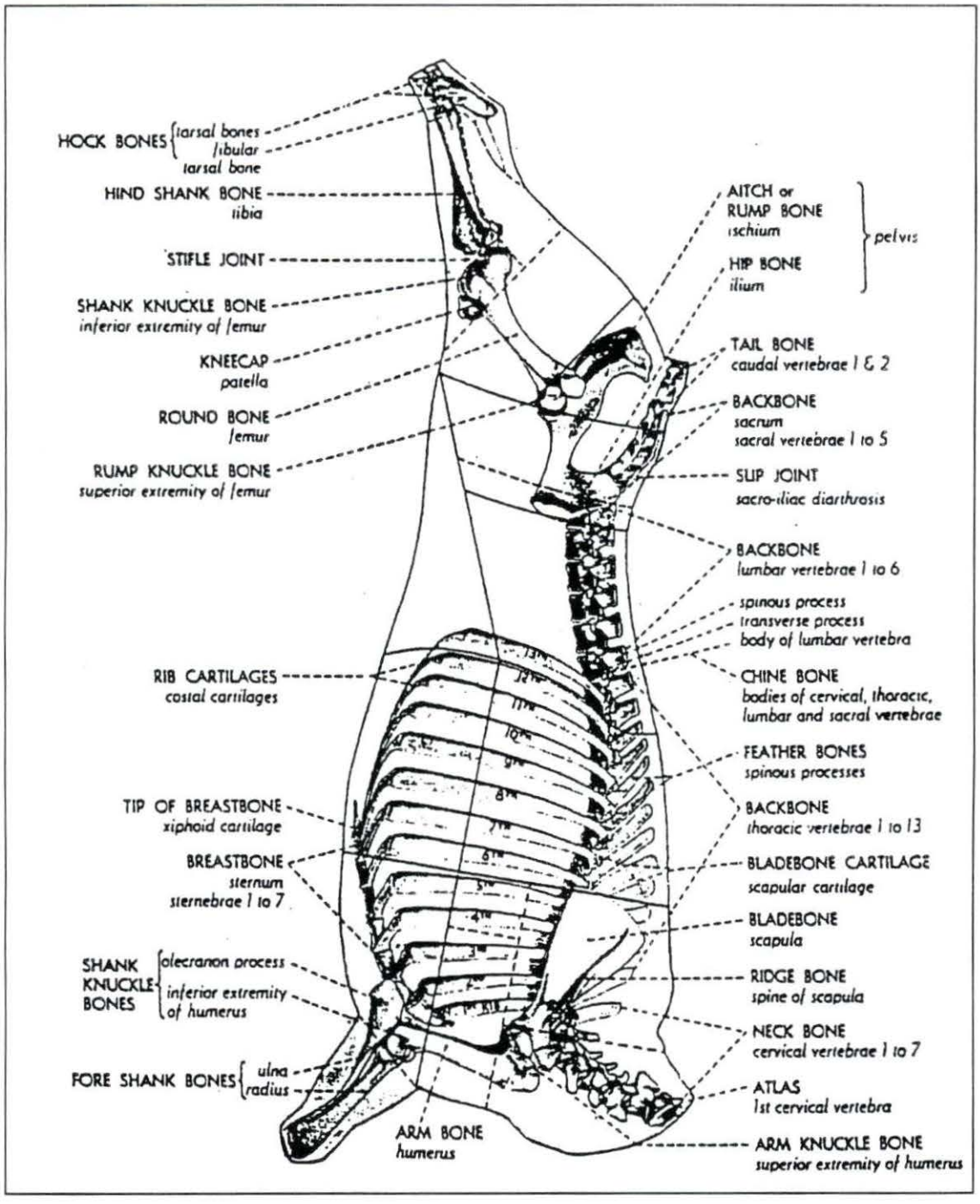

Figure B.1: Location of the bones of the split backbone of a beef carcass (Romans *et al.*, 1994).

Table B.1: Description of some beef carcass skeletal maturity characteristics for various maturities (Boggs and Merkel, 1980)

Maturity	Vertebrae			Ribs
	Sacral	Lumbar	Thoracic	
A^{0} to A^{30}	Distinct separation. Cartilage very evident	Cartilage evident on all vertebrae	Cartilage evident on all vertebrae: soft porous, and very red chine bones pearly white cartilages	Red and rounded, only slight tendency towards flatness
A^{90} to B^{30}	Completely fused	Nearly completely ossified, may be some cartilage	Slightly red and slightly soft chine bones - cartilage have some evidence of ossification	Slightly wide and slightly flat. Loss of some redness
B^{70} to B^{100}	Completely fused	Completely ossified	Chine bones tinged w/ red - cartilages are partially ossified; lower thoracic buttons show roughness	Slightly wide and flat. Slight flinty appearance
(maximum maturity for Prime, Choice, Select, and Standard grades)				
C^{0} to C^{30}	Completely fused	Completely ossified	Chine bones tinged w/ red - cartilages are partially to moderately ossified	Slightly wide and slightly flat. Somewhat bleached and slight flinty appearance
C^{70} to D^{40}	Completely fused	Completely ossified	Moderately hard, rather chine bones --cartilages show considerable ossification but outlines are plainly visible	Moderately wide flat, bleached and flinty
D^{50} to D^{100}	Completely fused	Completely ossified	Cartilages nearly completely ossified (70-100%). Fine outline still visible at the tips	Wide and flat
E^{0} to E^{30}	Completely fused	Completely ossified	Hard white chine bones; cartilages entirely ossified, outline barely visible	Wide and flat
E^{100}	Completely fused	Completely ossified	No visible outline of cartilage	Wide and flat

APPENDIX C

BILL OF MATERIALS OF THE INSTRUMENT

Table C.1: Parts list and bill of materials.

Bill of Materials

Item	Quantity	Reference	Price	Description
1	3	C1, C8, C9	0.30	22 pF, Ceramic Capacitor, 10%
2	1	C2	0.10	5 nF, Ceramic Capacitor, 10%
3	6	C3, C4, C6, C7, C10, C11	0.60	0.1 uF, Ceramic Capacitor, 20%
4	1	C5	0.10	1.5 pF, Ceramic Capacitor, 10%
5	1	C12	0.10	22 uF, Electrolytic Capacitor, 20%
6	2	D1, D2	0.10	1N4148, Diode
7	1	L1	0.15	13 uH, Inductor
8	1	L2	0.15	330 uH, Inductor
9	1	LCD	10.39	Liquid Crystal Display
10	2	Q1, Q2	0.30	2N2907A, PNP Transistor
11	2	Q3, Q4	0.30	2N3904, NPN Transistor
12	4	R1, R8, R9, R18	0.08	10 KΩ, Resistor, 1/4 W, 5%
13	2	R2, R4	0.04	500Ω, Potentiometer, 10 turns
14	3	R3, R16, R19	0.06	1 KΩ, Resistor, 1/4 W, 5%
15	3	R5, R13, R15	0.06	33 KΩ, Resistor, 1/4 W, 5%
16	1	R6	0.02	100 KΩ, Resistor, 1/4 W, 5%
17	1	R7	0.02	56 KΩ, Resistor, 1/4 W, 5%
18	2	R10, R17	0.04	10 KΩ, Potentiometer, 10 turns
19	2	R11, R12	0.04	1 MΩ, Potentiometer, 10 turns
20	1	R14	0.02	100 KΩ, Potentiometer, 10 turns
21	1	RCV	30.00	Receiver Transducer
22	1	TDX	30.00	Transmitter Transducer
23	1	U1	1.77	LM555C, Timer
24	1	U2	1.00	74HC221, Dual monostable
25	2	U3, U4	4.46	MAX903, Comparator
26	1	U5	0.58	74HC390, 4-bit Decade Counter
27	1	U6	3.72	25 MHz Crystal
28	1	U7	1.50	74C4543, BCD-to-7 Segment Latch/Decoder/Driver for LCD
29	1	U8	11.40	74C945, 4-digit Up/Down Counter /Latch/Decoder Driver for LCD/
30		U9	0.34	78LS05, +5 V Voltage Regulator
31	1	Batt	1.78	9 V Alkaline Battery
32	2	1 mt. Coax Cable	0.50	Coaxial cable for TDX and RCV
33	1	Box	6.44	Plastic enclosure
34	1	Caliper	30.00	Calibrated Caliper
		Total cost	**$ 136.46**	

APPENDIX D

STATISTICAL ANALYSIS SUMMARY

Table D.1: Rearranged data for the repeatability and reliability study.

Bone 1 Samples 1&2					
0.904	**0.905**	**0.906**	**0.907**	**0.908**	**0.909**
3021	3041	3028	3015	3035	3038
3005	3025	3028	3015	3019	3022
2974	3009	2996	3015	3003	3006
2959	3009	2996	3000	3003	2991
2929	2993	2981	3000	2987	2975
.	2978	2981	3000	2987	2975
.	2962	2981	3000	2987	2960
.	2962	2966	2984	2987	2960
.	2947	2950	2984	2957	2945
.	2947	2950	2984	2957	2930
.	.	2935	2984	2957	.
.	.	2935	2984	2942	.
.	.	2920	2984	2942	.
.	.	2920	2984	2942	.
.	.	2906	2969	2927	.
.	.	.	2954	.	.
.	.	.	2954	.	.
.	.	.	2938	.	.
.	.	.	2938	.	.
.	.	.	2938	.	.
.	.	.	2938	.	.
.	.	.	2924	.	.
.	.	.	2894	.	.

Bone 2 Samples 3&4						
0.773	**0.774**	**0.775**	**0.776**	**0.777**	**0.778**	**0.779**
3068	3072	3095	3061	3084	3069	3111
3049	3053	3076	3061	3065	3050	3111
3049	3034	3076	3061	3065	3031	3072
3030	3034	3038	3042	3027	3031	3053
3011	3034	3019	3042	3027	3012	3053
3011	3034	3001	3042	3009	3012	3035
2975	3015	3001	3042	3009	3012	3035
2904	3015	2983	3042	3009	2994	3016
.	3015	2983	3023	3009	2958	2998
.	3015	2965	3005	2990	.	2998
.	2979	.	3005	2990	.	2998
.	.	.	3005	2937	.	2980
.	.	.	3005	.	.	.

Bone 3 Samples 5&6					
0.769	**0.770**	**0.771**	**0.772**	**0.773**	**0.774**
2924	2963	2949	2935	2957	2943
2924	2945	2932	2935	2922	2943
2907	2945	2932	2935	2887	2926
2907	2928	2932	2935	2887	2926
2907	2910	2914	2935	2870	2908
2889	2910	2914	2918	2854	2908
2889	2893	2897	2918	2837	2891
2872	2876	2897	2918	.	2874
2872	2876	2897	2901	.	2858
2839	2876	2897	2901	.	.
2839	2876	2880	2901	.	.
2839	2843	2880	2901	.	.
.	.	2863	2901	.	.
.	.	.	2901	.	.
.	.	.	2884	.	.
.	.	.	2867	.	.
.	.	.	2867	.	.

Bone 1 (Samples 1&2)

Duncan's Multiple Range Test for variable: Speed of Sound

Alpha = 0.05 df = 72 MSE = 1161.78

Harmonic Mean of cell sizes = 10.40

Number of Means	2	3	4	5	6
Critical Range	29.79	31.35	32.37	33.12	33.70

Means with the same letter are not significantly different.

Duncan Grouping	Mean	N	Distance
A	2987.21	10	d2
A	2980.30	10	d6
A	2977.76	15	d1
A	2975.44	15	d5
A	2973.14	23	d4
A	2964.96	15	d3

Bone 2 (Samples 3&4)

Duncan's Multiple Range Test for variable: Speed of Sound

Alpha = 0.05 df = 68 MSE = 1410.02

Harmonic Mean of cell sizes = 10.49

Number of Means	2	3	4	5	6	7
Critical Range	32.80	34.51	35.64	36.46	37.10	37.61

Means with the same letter are not significantly different.

Duncan Grouping	Mean	N	Distance
A	3038.46	12	d7
A	3033.22	13	d4
A	3027.27	11	d2
A	3023.51	10	d3
A	3018.83	9	d6
A	3018.19	12	d5
A	3012.20	8	d1

Bone 3 (Samples 5&6)

Duncan's Multiple Range Test for variable: Speed of Sound

Alpha = 0.05 df = 64 MSE = 914.99

Harmonic Mean of cell sizes = 10.78

Number of Means	2	3	4	5	6
Critical Range	26.02	27.38	28.27	28.92	29.43

Means with the same letter are not significantly different.

Duncan Grouping	Mean	N	Distance
A	2908.96	17	d4
A	2908.49	9	d6
A	2906.42	13	d3
A	2903.63	12	d2
A	2887.89	7	d5
A	2884.03	12	d1

Figure D.1: Summary of the SAS output for the multiple comparison test.

Correlation Analysis for Bone 1 (Samples 1&2)
Cronbach Coefficient Alpha

for RAW variables 0.896
for STANDARDIZED variables 0.991

	Raw Variables		Std. Variables	
Deleted Variable	Correlation with Total	Alpha	Correlation with Total	Alpha
S1	0.610	0.896	0.971	0.989
S2	0.811	0.864	0.971	0.989
S3	0.819	0.862	0.985	0.987
S4	0.395	0.923	0.912	0.994
S5	0.853	0.859	0.978	0.988
S6	0.879	0.853	0.990	0.987

Correlation Analysis for Bone 2 (Samples 3&4)
Cronbach Coefficient Alpha

for RAW variables 0.933
for STANDARDIZED variables 0.979

	Raw Variables		Std. Variables	
Deleted Variable	Correlation with Total	Alpha	Correlation with Total	Alpha
S1	0.701	0.940	0.844	0.980
S2	0.797	0.927	0.898	0.977
S3	0.921	0.908	0.971	0.971
S4	0.721	0.933	0.887	0.977
S5	0.837	0.917	0.930	0.974
S6	0.800	0.922	0.938	0.974
S7	0.967	0.903	0.969	0.972

Correlation Analysis for Bone 3 (Samples 5&6)
Cronbach Coefficient Alpha

for RAW variables 0.904
for STANDARDIZED variables 0.984

	Raw Variables		Std. Variables	
Deleted Variable	Correlation with Total	Alpha	Correlation with Total	Alpha
S1	0.785	0.880	0.967	0.979
S2	0.94	0.852	0.969	0.979
S3	0.878	0.874	0.958	0.980
S4	0.584	0.908	0.882	0.987
S5	0.596	0.920	0.923	0.983
S6	0.776	0.882	0.976	0.978

Figure D.2: Summary of the SAS output for the calculation of the reliability coefficient (Cronbach's alpha).

Table D.2: Summary of the SAS output for the comparison of the two age groups (15 and 48 months) in experiment one.

t-Test: Two-Sample Assuming Unequal Variances		
	15 months	*48 months*
Mean	2506.7	2918.1
Variance	21428.9	4041.6
Observations	30	50
Hypothesized Mean Difference	0	
df	36	
t Stat	-14.59	
P(T<=t) one-tail	<0.0001	

Table D.3: Summary of the SAS output for the linear regression for experiment one.

Regression Statistics	
Multiple R	0.8915
R Square	0.7948
Adjusted R Square	0.7921
Standard Error	7.3287
Observations	80

ANOVA

	df	*SS*	*MS*	*F*	*Significance F*
Regression	1	16229.39	16229.39	302.17	<0.0001
Residual	78	4189.36	53.71		
Total	79	20418.75			

	Coefficients	*Standard Error*	*t Stat*	*P-value*
Intercept	-140.55	10.17	-13.83	<0.0001
Speed	0.064	0.0037	17.38	<0.0001

Experiment two: Difference with respect to Age
Duncan's Multiple Range Test for variable: Speed of Sound
Alpha = 0.05 df =153 MSE = 11569.04
Harmonic Mean of cell sizes =32

Number of Means	2	3	4
Critical Range	53.12	55.92	57.78

Means with the same letter are not significantly different.

Duncan Grouping		Mean	N	Age
	A	2879.33	48	36
B	A	2850.50	48	30
B	A	2839.50	16	45
B		2807.04	48	18

Experiment two: Difference with respect to Anatomical Plane
Duncan's Multiple Range Test for variable: Speed of Sound
Alpha = 0.05 df =153 MSE = 11569.04

Number of Means	2	3	4
Critical Range	47.52	50.015	51.685

Means with the same letter are not significantly different.

Duncan Grouping	Mean	N	Anatomical Plane
A	2891.43	40	Anterior
B	2837.83	40	Posterior
B	2829.38	40	Medial
B	2821.43	40	Lateral

Figure D.3: Summary of the SAS output for the comparison of the speed of sound at different anatomical planes and at different skeletal maturity stages in experiment two.

Table D.4: Linear regression summary for the right humerus.

Regression Statistics	
Multiple R	0.9441
R Square	0.8913
Adjusted R Square	0.8875
Standard Error	2.55
Observations	60

ANOVA

	df	*SS*	*MS*	*F*	*Significance F*
Regression	2	3040.99	1520.49	233.77	<0.0001
Residual	57	370.75	6.50		
Total	59	3411.73			

	Coefficients	*Standard Error*	*t Stat*	*P-value*
Intercept	-56.88	8.48	-6.71	<0.0001
Weight	0.029	0.0031	9.32	<0.0001
Speed	0.014	0.0038	3.70	0.0005

Table D.5: Linear regression summary for the left humerus.

Regression Statistics	
Multiple R	0.9249
R Square	0.8554
Adjusted R Square	0.8493
Standard Error	2.69
Observations	50

ANOVA

	df	*SS*	*MS*	*F*	*Significance F*
Regression	2	2015.66	1007.83	139.0	<0.0001
Residual	47	340.66	7.25		
Total	49	2356.32			

	Coefficients	*Standard Error*	*t Stat*	*P-value*
Intercept	-49.67	9.99	-4.97	<0.0001
Weight	0.034	0.0030	11.46	<0.0001
Speed	0.009	0.0040	2.37	0.0217

Table D.6: Linear regression summary for the right femur.

Regression Statistics	
Multiple R	0.9351
R Square	0.8744
Adjusted R Square	0.8712
Standard Error	2.58
Observations	80

ANOVA

	df	*SS*	*MS*	*F*	*Significance F*
Regression	2	3570.49	1785.24	268.11	<0.0001
Residual	77	512.71	6.66		
Total	79	4083.20			

	Coefficients	*Standard Error*	*t Stat*	*P-value*
Intercept	-60.90	10.13	-6.01	<0.0001
Weight	0.033	0.0023	14.27	<0.0001
Speed	0.014	0.0040	3.49	0.0008

Table D.7: Linear regression summary for the left femur.

Regression Statistics	
Multiple R	0.9287
R Square	0.8624
Adjusted R Square	0.8589
Standard Error	2.70
Observations	80

ANOVA

	df	*SS*	*MS*	*F*	*Significance F*
Regression	2	3521.54	1760.77	241.39	<0.0001
Residual	77	561.66	7.29		
Total	79	4083.20			

	Coefficients	*Standard Error*	*t Stat*	*P-value*
Intercept	-48.86	10.98	-4.45	<0.0001
Weight	0.030	0.0041	7.47	<0.0001
Speed	0.011	0.0050	2.11	0.0384